fibers

MDPI

Article

Enhancing Interfacial Adhesion in Kevlar and Ultra-High Molecular Weight Polyethylene Fiber-Reinforced Laminates: A Comparative Study of Surface Roughening, Plasma Treatment, and Chemical Functionalization Using Graphene Nanoparticles

Feyi Adekunle [1], Jan Genzer [2] and Abdel-Fattah M. Seyam [1,*]

[1] Department of Textile and Apparel, Technology and Management, Wilson College of Textiles, North Carolina State University, Raleigh, NC 27606, USA; ohadekun@ncsu.edu
[2] Department of Chemical & Biomolecular Engineering, North Carolina State University, Raleigh, NC 27695, USA; jgenzer@ncsu.edu
* Correspondence: aseyam@ncsu.edu

Abstract: This study investigates the impact of mechanical and chemical surface treatments on the interfacial adhesion and mechanical properties of Kevlar and ultra-high molecular weight polyethylene (UHMWPE) fiber-reinforced laminates (FRLs). Various treatments, including surface roughening, plasma exposure, NaOH and silane coupling, and graphene nanoparticle (NP) incorporation, were conducted to enhance the fiber–matrix bonding within thermoplastic polyurethane (TPU) and ethylene-vinyl acetate (EVA) matrices. Results demonstrated that treatment efficacy highly depends on fiber type and matrix material, with chemical modifications generally outperforming the physical treatment (surface roughness). Plasma treatment significantly enhanced adhesion for UHMWPE, increasing yarn pullout force by 188.1% with TPU. While combining plasma with graphene slightly improved performance, it did not exceed plasma-only results due to potential surface functionalization losses during wet graphene application. For Kevlar, the combination of NaOH, silane, and graphene NP (NSG) treatment yielded the highest adhesion, showing increases of 76.6% with TPU and 95.4% with EVA, underscoring the synergy between chemical coupling and nanomaterial reinforcement. This study's insights align with previous research, expanding the knowledge base by investigating graphene's role independently and alongside established methods.

Keywords: fiber-reinforced laminate (FRLs); Kevlar; ultra-high molecular weight polyethylene (UHMWPE); interfacial adhesion; surface roughening; plasma treatment; chemical functionalization; yarn pullout in laminate test

check for updates

Academic Editor: Martin J. D. Clift

Received: 21 November 2024
Revised: 23 January 2025
Accepted: 7 February 2025
Published: 11 February 2025

Citation: Adekunle, F.; Genzer, J.; Seyam, A.-F.M. Enhancing Interfacial Adhesion in Kevlar and Ultra-High Molecular Weight Polyethylene Fiber-Reinforced Laminates: A Comparative Study of Surface Roughening, Plasma Treatment, and Chemical Functionalization Using Graphene Nanoparticles. *Fibers* **2025**, *13*, 19. https://doi.org/10.3390/fib13020019

Copyright: © 2025 by the authors. Licensee MDPI, Basel, Switzerland. This article is an open access article distributed under the terms and conditions of the Creative Commons Attribution (CC BY) license (https://creativecommons.org/licenses/by/4.0/).

1. Introduction

Fiber-reinforced laminates (FRLs) are used in high-performance applications in aerospace (e.g., aircraft fuselage panels, satellite components, technical inflatables), automotive (e.g., crash-resistant panels, lightweight structural reinforcements), and naval applications (e.g., hulls for high-speed vessels due to their exceptional mechanical properties, high strength-to-weight ratios, durability, and resistance to extreme conditions). Kevlar and UHMWPE fibers are among the most commonly used high-performance fibers in laminates due to their exceptional tensile strength, chemical resistance, and impact toughness [1–4]. However, due to the fibers' inert and highly crystalline nature, a critical challenge in optimizing the performance of FRLs lies in enhancing the interfacial adhesion

between the fibers, the surrounding polymer matrix, and the backing material [5]. Moreover, poor interfacial strength also directly influences the mechanical properties of the composites; it can lead to premature failure, reducing the mechanical efficiency and long-term reliability of the laminate structure and ultimately causing rupture of the inflatables [6,7].

To improve interfacial adhesion, researchers have explored both mechanical and chemical surface treatments to enhance fiber–matrix bonding [5,8–10]. On the one hand, mechanical surface treatments, such as increasing surface roughness, can increase the available contact area and promote mechanical interlocking between the fiber and adhesive [11]. On the other hand, chemical treatments modify the fiber surface at the molecular level by introducing functional groups that enhance chemical bonding between the fibers and the matrix. Multiple surface treatment techniques, including plasma treatments, chemical treatments, coatings, and methods such as ultraviolet (UV) and gamma irradiation, have enhanced the interfacial properties of fiber-reinforced materials. In recent years, the innovative use of nanoparticles, particularly graphene nanoparticles, in composite materials has greatly garnered attention for enhancing interfacial adhesion [12]. This promising approach holds the potential to significantly advance interfacial bonding in fiber-reinforced laminates (FRLs), representing a significant breakthrough in the field.

Physical surface treatment methods, e.g., roughening and abrasion, offer several advantages over chemical methods. They are typically more straightforward and more easily controlled, allowing for consistent modification without requiring complex chemical reactions or specialized equipment [12]. Additionally, physical techniques do not involve harsh chemicals that might damage the fiber's inherent properties, making them a safer option for preserving the material's integrity. However, while physical treatments can increase surface roughness and promote mechanical interlocking, they may not achieve the same level of strong interfacial adhesion as chemical methods [13]. Nonetheless, their cost-effectiveness and reduced environmental impact make them attractive for enhancing the fiber–matrix interface. Wu et al. [14] demonstrated that mechanical abrasion significantly affects surface properties, enhancing surface roughness and promoting better mechanical interlocking and adhesive infiltration. In their study, fiber metal laminates (FMLs) treated with sandpaper exhibited increased lap shear strength compared to untreated surfaces. While mechanical treatments such as sanding enhance adhesion by altering surface topography, they are often supplemented with chemical treatments to introduce functional groups that improve bonding on a molecular level.

Plasma treatment has been extensively studied as an effective method for modifying fiber surfaces. It simultaneously roughens the fiber surface and introduces chemical functionalities, enhancing mechanical interlocking and chemical bonding. Plasma has been created using a variety of gases, including oxygen, nitrogen, helium, and air [15–17]. The produced gas ions collide with the exposed sample, changing the surface's chemical composition and landscape. The rupturing of chemical bonds and the creation of free radicals are included in these chemical changes. The surface entities that have been activated may then be joined with the excited ions or cross-linked to form chemically reactive functional groups. While plasma etching and overheating improved the adhesion of fibers to polymer matrices by introducing polar groups such as hydroxyl, ether, and carbonyl on the outer layer of the fibers' surface without affecting its bulk properties, micro-pits can also be created as a result [18]. Unlike Kevlar, which contains amide groups and a few hydrogen bonds, UHMWPE fibers lack reactive sites, making plasma treatment one of the few viable methods to modify their surface chemically. Liu et al. introduced oxygen-based functional groups onto the surface of UHMWPE using oxygen plasma treatment, which significantly improved its wettability and its tribological properties [19]. Another study by Teodoru et al. employed atmospheric pressure dielectric barrier discharge (DBD)

plasma treatment with various gases (Ar, He, He/O_2, N_2, and O_2) to modify the surface of UHMWPE fibers continuously. Characterization using FTIR, XPS, and AFM revealed increased oxygen-containing functional groups, enhanced cross-linking, and varied surface roughness. Adhesion tests also showed that the plasma treatment provided a higher adhesive strength with epoxy [16]. While plasma treatment is often described as a physical method due to its ability to roughen fiber surfaces, it is equally important to recognize its role as a chemical treatment [20–22]. Plasma introduces reactive species, such as ions, radicals, and ultraviolet photons, which interact with the fiber surface to modify its chemical structure. These interactions can break molecular bonds, create new functional groups (e.g., hydroxyl, carboxyl, or carbonyl groups), and enhance the fiber's ability to form chemical bonds with the polymer matrix [15,16,19,23]. Thus, plasma treatment affects the surface's physical morphology and alters its chemical composition, making it a hybrid process that improves adhesion through mechanical and chemical mechanisms. Other chemical treatments, i.e., NaOH and silane coupling agents, have been more thoroughly explored for Kevlar fibers. Alkaline NaOH solutions alter the fiber surface by hydrolyzing the surface layers and exposing functional groups that promote adhesion. When combined with silane treatment, a coupling agent that forms covalent bonds with the fiber and matrix, these modifications can significantly increase the adhesion between Kevlar fibers and the polymer matrix. The literature has shown that pre-treating fibers with NaOH before grafting silane leads to enhanced bonding efficiency. Multiple studies have investigated how the surface of the Kevlar fibers is modified with 3-aminopropyltriethoxysilane (APTES) by condensation between the Si-OH on the surface of the Kevlar fabric and the siloxane from the silane coupling agent [1,5,10,11,24,25]. They have found that this treatment produces an amine-functionalized Kevlar surface that increases the interfacial shear strength (IFSS) of the poly-p-phenylene-benzimidazole-terephthalamide fiber/epoxy matrix by 46.7% [24,25]. Kim et al. [26] observed that the flame treatment of a Kevlar fiber composite with 0.5 wt% of APTES and 3-methacryloxypropyltrimethoxysilane (APTMS) increased its single-lap adhesive strength. As a result, the treatment enhanced the bonding between the C=O of APTMS and -N-H of APTES. Ramasamy et al. [27] also investigated the modification of Kevlar with various silane treatments. A 1 wt% 3-APTES silane coupling agent mixed with an acidic solution, as well as a mixture of 0.5 wt% APTES and 0.5 wt% APTMS, and 0.5 wt% of nano-SiO_2 were all used in treating Kevlar fibers. These treatments led to improved adhesion, higher tensile strength, tensile modulus, flexural modulus, and flexural strength; however, pretreating the fibers with sodium hydroxide, phosphoric acid, and/or maleic anhydride led to even better results than with just the silane agents alone.

In contrast to these established methods, the grafting of nanoparticles onto fiber surfaces is a relatively novel approach, with only a few studies exploring its potential for improving interfacial adhesion [12,13,28–32]. Because of their excellent mechanical and physical qualities, nano-reinforcements such as carbon nanotubes, nanoclay, carbon nanofibers, and graphene nanoparticles have been frequently employed to alter polymer matrices. Graphene nanoparticles (NPs), in particular, have recently been investigated as a potential nano-reinforcement for modifying the chemistry of polymer matrices and improving adherence [12,13,33,34]. Known for its unique structural, electrical, and mechanical properties, graphene can introduce surface functionalization without physically degrading the fibers. This opens up new possibilities for enhancing the performance of FRLs.

Chowdhury et al. [13] investigated the effects of depositing graphene nanoparticles on Kevlar fabrics via a dip coating process. They found that since nanoparticles alone tend to aggregate due to attractive forces, adding a binder improves the deposition and increases adhesion at the interface. They also found that with the deposition of the graphene nanoparticles, the interfacial adhesion was enhanced, and the decomposition temperature

and mechanical properties also improved significantly and were superior to the untreated fabric. The improved adhesion in Kevlar fibers coated with graphene NPs [13] is due to an atomic bonding mechanism. Kevlar fibers possess large, parallel molecular chains with a crystalline structure, leading to anisotropic properties. NPs, with their distinct crystalline structure, form chemical bonds with the Kevlar surface through a functionalization process. This involves chemical reactions between the nanoparticles and the fiber surface, creating hardened bonds between the adhesive molecules and Kevlar. Additionally, graphene's large surface area increases the contact area between the substrate and adhesive, significantly improving adhesion [34]. Graphene oxide also boosts shear strength at the interface due to strong interactions between the oxygen-containing functional groups of graphene oxide and the epoxy resin. The large surface area and high aspect ratio of graphene oxide provide additional bonding sites for the adhesive, further enhancing interfacial strength.

Moreover, research by Xu et al. demonstrates that graphene NPs can create a robust interface with epoxy resin due to the active groups on their surface [35]. These active groups allow external forces to be transferred from the nanoparticles to the surrounding area, causing microcracks in the epoxy resin matrix, which absorb energy. Additionally, nanoparticles serve as physical cross-linking points for molecular chains, preventing the microcracks from spreading and enhancing the overall integrity of the material [35]. Graphene NPs enhance the adhesive bond's shear strength through increased surface area and effective dispersion within the epoxy matrix. This enables efficient stress transmission from the adhesive to the substrate, improving adhesion. Tan et al. [33] also explored the effect of graphene on the yarn pullout force and ballistic performance of Kevlar textiles impregnated with shear thickening fluids (STFs). The testing method used by Tan et al. is similar to the approach in the current study, as both assess the pullout force of yarns to measure interfacial adhesion. However, the critical difference is that the former was conducted on a fabric sample with a much longer gauge length, while our study focuses on measuring adhesion within a fiber-reinforced laminate (FRL) material. Despite this difference, the similarity in setup allows us to draw meaningful conclusions about the efficacy of graphene in enhancing interfacial adhesion, providing valuable insights for our study. The findings indicated that STF reinforced with graphene prevents the yarns from sliding better than pure STF, and the single yarn pullout force is almost five times higher with the addition of the graphene NPs. The enhanced contact between the graphene–STF/Kevlar fabric yarns leads to coupling integration, allowing more fibers to be linked together to withstand external impact loading.

While using nanoparticles in composite materials has shown promising results in enhancing interfacial adhesion, their application in fiber-reinforced laminates (FRLs) remains relatively novel and under investigation. The novelty of our study lies in the exploration of graphene nanoparticles, specifically in FRLs, which are thinner and more flexible than other composite materials. Furthermore, limited research has focused on combining nanoparticles with different surface treatments, and no other studies have utilized the innovative yarn pullout in laminate test, a method tailored to assess FRLs. Given the differences in chemical reactivity and structural properties between Kevlar and UHMWPE fibers, this study aims to systematically evaluate the effects of mechanical and chemical surface treatments, including surface roughness, plasma treatment, NaOH + silane treatment, and graphene nanoparticles. By doing so, we seek to deepen the understanding of fiber–matrix adhesion in these materials and contribute to developing more durable and high-performing laminated composites. The subsequent sections of this paper are organized as follows: Section 2 details the experimental procedures, including the plasma treatment setup, surface characterization techniques, and adhesion testing methodology. Section 3 presents and discusses the results, focusing on the chemical and morphological

changes induced by plasma treatments and their effects on adhesion. Finally, Section 4 provides concluding remarks, summarizing key findings and their implications for the improved adhesion properties of UHMWPE fibers.

2. Materials and Methods

2.1. Materials

This study utilized Kevlar (CST, Tehachapi, CA, USA) and UHMWPE fibers (Zhejiang Mengtex Special Materials Technology Co., Ltd., Jiaxing, China) as reinforcements for the fiber-reinforced laminates. Kevlar and ultra-high molecular weight polyethylene (UHMWPE) were chosen for this study due to their widespread use in high-performance fiber-reinforced composites. Kevlar is well-known for its exceptional strength-to-weight ratio, high tensile strength, and heat resistance, making it ideal for ballistic protection, aerospace, and industrial applications. UHMWPE also offers superior impact resistance, lightweight properties, and chemical resistance. Both fibers, however, present adhesion challenges due to their chemically inert surfaces, necessitating advanced surface treatments to enhance bonding with polymer matrices in composite structures. The laminate was constructed inhouse at the Wilson College of Textiles using Mylar film (CS Hyde, Lake Villa, IL, USA) with two adhesive layers encasing the central load-bearing layer, as seen in Figure 1. The treated and untreated (control) samples were incorporated into the matrices using a hand layup method. The fabric and adhesive were alternately stacked: a layer of the adhesive film, then a layer of the fabric, another adhesive layer, and finally, the mylar film. The laminates were run through a Pratix OK-12L seamless Teflon belt drum laminator at the respective adhesive melting temperatures with a double-pass method to ensure proper adhesive melting. The temperature was set to 100 °C for EVA samples and 110 °C for TPU samples. The feed speed was maintained at 0.32 m/min with a pressure of 413.685 kPa (60 psi). The final laminate thickness was approximately 3 mm. Graphene nanopowder, with a particle size of 5–10 nm (purchased from Sigma-Aldrich), was used for surface functionalization of the fibers and adhered using a Polyvinyl Alcohol (PVA) solution (ALDON, Avon, NY, USA). Sodium hydroxide (NaOH, XFNANO, Pukou, Nanjing, China) was employed for the alkali treatment of Kevlar fibers, while nano-SiO_2 and APTES (Spectrum Chemical, Dawsonville, GA, USA) were utilized as silane coupling agents. Additionally, ethylene-vinyl acetate (EVA) and thermoplastic polyurethane (TPU) adhesives (both from KETAEBO, Suzhou, China) were selected for their complementary properties, making them suitable for bonding fiber-reinforced laminates. EVA is known for its flexibility, good adhesion to various surfaces, and impact resistance, making it ideal for applications requiring durability and elasticity. TPU offers excellent mechanical properties, including high tensile strength, abrasion resistance, and the ability to maintain flexibility at low temperatures. Both adhesives are also commonly used in industry, particularly in fiber-reinforced laminated materials, due to their reliability and performance in enhancing interfacial adhesion between fibers and polymer matrices. The selected laminate design follows the traditional structural and material configuration used in laminate materials for inflatable structures like airships, aerostats, inflatable antennas, and similar applications. Additionally, it is well-suited for evaluating the adhesion strength between the fiber and film layers. The laminate structure is illustrated in Figure 1. All chemical treatments described in this study were developed in-house to ensure precise control over treatment parameters and compatibility with the experimental setup.

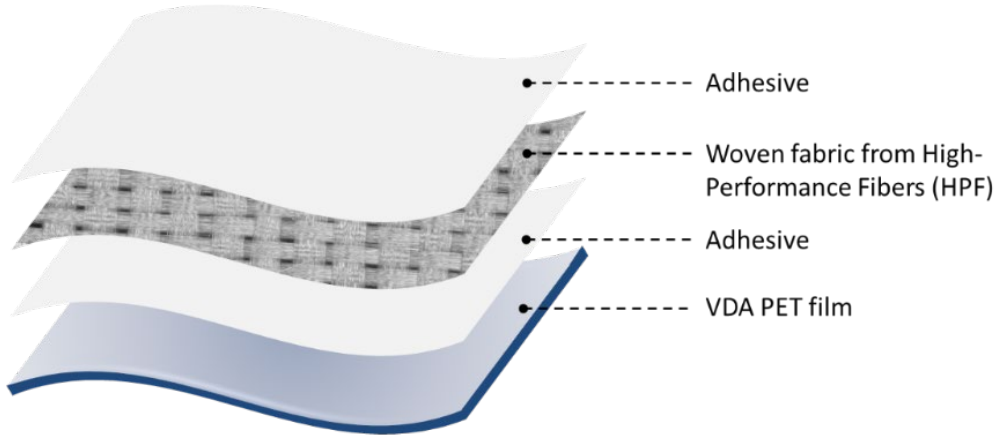


Figure 1. Fiber-reinforced laminate structure.

2.2. Physical Treatment

The surface roughening of the fabrics was conducted using a Wyzenbeek Oscillatory Cylinder Abrasion Tester following ASTM D4157-13 [36] (Reapproved in 2022)—"Standard Test Method for Abrasion Resistance of Textile Fabrics (Oscillatory Cylinder Method)". Figure 2 displays the setup. Although this method is traditionally used to measure abrasion resistance through a unidirectional rubbing action, it was adapted to introduce surface roughening to the surface of the HPF fabrics. The treatment area (70 mm × 70 mm) was confined to the area in the red square in Figure 2.

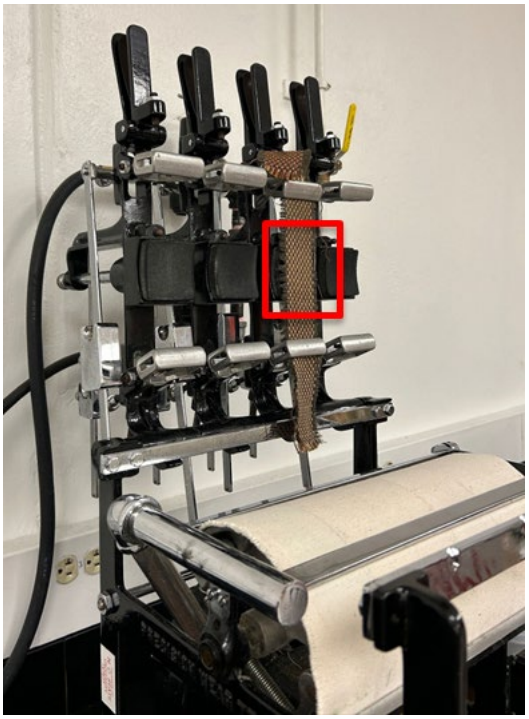
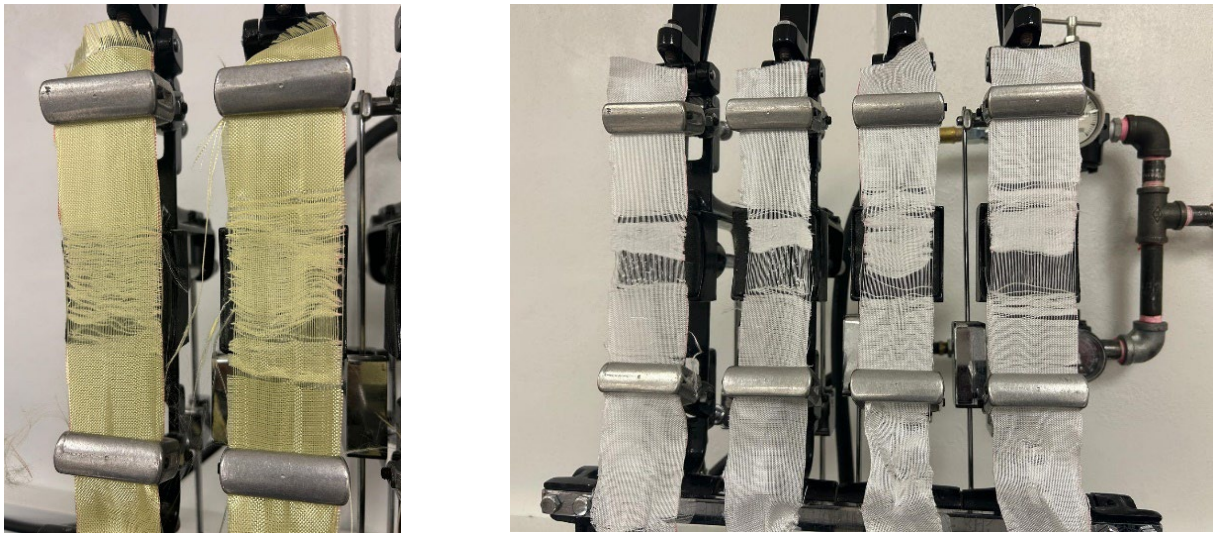


Figure 2. Wyzenbeek Oscillatory Cylinder Abrasion Tester setup for surface roughening of high-performance fabrics. The red square indicates the 70 mm × 70 mm treatment area.

Specimens measuring 70 mm × 245 mm were prepared from each fabric roll in warp and weft directions. The specimens were mounted on the abrasion tester, where the testing area was rubbed with controlled pressure and tension. The machine was calibrated to oscillate through a 76 mm arc. Preliminary trials were conducted using various abrasive materials, including metal sheets, grit sandpapers, and cotton duck fabrics.

Each fabric sample was exposed to these abrasives over varying cycles to determine the optimal conditions for surface roughening. The preliminary observations showed that the sandpapers and the metal sheets used to abrade the fibers mechanically were too rough, leading to excessive material removal and shifting of the fibers during treatment, as can be seen in Figures 3a and 3b for Kevlar and UHMWPE, respectively.



(**a**) (**b**)

Figure 3. Fiber shifting in fabric samples after abrasive treatment using sandpapers and metal sheets for (**a**) Kevlar and (**b**) UHMWPE.

Cotton duck fabric was used to achieve a gentler surface roughening, allowing for more controlled abrasion without significantly displacing the fibers. The test was conducted for 250 cycles, which was determined to provide sufficient surface modification without over-abrading the fabric. Following abrasive treatment, the surface morphology was examined to assess the effects of roughening. The fabrics were then cleaned with ethanol and left to dry at room temperature overnight to remove any debris before further testing. The samples used in this study were classified based on the type of fiber (Kevlar or UHMWPE), the matrix material (EVA or TPU), and whether the sample was untreated (control) or treated with surface roughening. Kevlar samples are denoted by the prefix KP60, while UP66 represents UHMWPE samples. The matrix type is indicated by either EVA (ethylene-vinyl acetate) or TPU (thermoplastic polyurethane). The suffix C represents control samples (untreated), and T indicates treated samples (subjected to physical roughening). These details of the fabric parameters and sample identification are enumerated in Table 1.

Table 1. Fabric parameters and sample identification for physical surface roughening treatments.

Fiber Type	Fabric Areal Density (g/m^2)	Fabric Count (Ends/cm × Picks/cm)	Adhesive Type	Treatment	Sample ID
Kevlar	60	13.5 × 13.5	TPU	Control	K_TPU_C
Kevlar	60	13.5 × 13.5	TPU	Roughening	K_TPU_R
Kevlar	60	13.5 × 13.5	EVA	Control	K_EVA_C
Kevlar	60	13.5 × 13.5	EVA	Roughening	K_EVA_R
UHMWPE	66	15.7 × 11.8	TPU	Control	U_TPU_C
UHMWPE	66	15.7 × 11.8	TPU	Roughening	U_TPU_R
UHMWPE	66	15.7 × 11.8	EVA	Control	U_EVA_C
UHMWPE	66	15.7 × 11.8	EVA	Roughening	U_EVA_R

The surface morphologies of both untreated and treated fibers (Kevlar and UHMWPE) were analyzed using scanning electron microscopy (Hitachi TM4000 SEM, Krefeld, Germany) to assess surface roughness and topography changes visually. After roughening and treatment, fiber samples were mounted onto slides and SEM images were captured at various magnifications to provide detailed insight into the surface structure. Key regions of interest were selected along the fiber length, focusing on areas that displayed the most significant changes post-treatment. The roughness and texture of the fibers were qualitatively evaluated based on the visual differences in surface morphology between the untreated and treated samples. The images were used to highlight the effects of mechanical abrasion and chemical treatment on the fibers' surface roughness, explicitly looking for increases in surface irregularities, grooves, and fibrillation, contributing to improved adhesion in fiber-reinforced laminates.

2.3. Chemical Treatment (UHMWPE)

Plasma equipment: Plasma treatment was carried out using a low-pressure plasma chamber (Werner Mathis A.G. Model CH-8155) with a gas mixture of argon and oxygen (70:30 ratio). The pressure inside the chamber was maintained at 0.3 mbar, and the fibers were exposed to plasma for 5 min at 50 W of power. The 10 cm × 10 cm UHMWPE fabric swatches were placed in the plasma chamber, carefully centered to ensure uniform exposure to the plasma. The fabrics were laminated within 10–20 min after treatment to prevent contamination and preserve the potency of the plasma treatment.

2.4. Chemical Treatments (Kevlar)

NaOH treatment: the Kevlar fabrics were hydrolyzed in a 10 wt% aqueous NaOH solution for 30 min at room temperature, then thoroughly washed with distilled water and left to dry at room temperature for 24 h.

Silane treatment: Following the NaOH treatment, the Kevlar fabric swatches were immersed in a solution containing 0.5 wt% nano-SiO_2 mixed with 1 wt% APTES in anhydrous toluene. The fabrics were kept in the solution overnight at 50 °C in a liquid bath, as shown in Figure 4. Afterward, the swatches were dried in a vacuum oven at 110 °C for 2 h to complete the silane grafting process. Finally, they were washed with distilled water and left to dry overnight at room temperature.

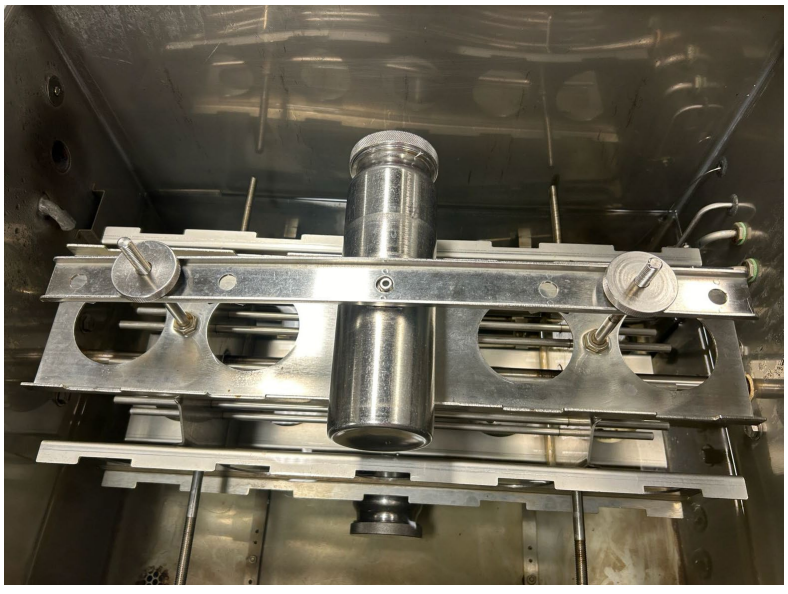


Figure 4. Liquid bath setup for silane treatment.

Graphene Nanoparticle Treatment

Graphene dispersion: 2 wt% graphene nanoparticles were dispersed in ethanol using ultrasonication at 100 W for 1 h to obtain a stable suspension. The fabric swatches were then submerged in the graphene dispersion for 30 min to allow nanoparticle attachment to the fiber surface. After graphene deposition, the fabrics were removed from the suspension, dried at 80 °C for 1 h in a vacuum oven, and inspected under scanning electron microscopy (SEM) to confirm the presence of nanoparticles on the fiber surface. The summary of the sample identification of all the chemically treated samples is summarized in Table 2.

Table 2. Fabric parameters and sample identification for chemical treatments.

Fiber Type	Fabric Areal Density (g/m^2)	Fabric Count (Ends/cm × Picks/cm)	Adhesive Type	Treatment	Sample ID
Kevlar	60	13.5 × 13.5	TPU	Control	K_TPU_C
Kevlar	60	13.5 × 13.5	EVA	Control	K_EVA_C
Kevlar	60	13.5 × 13.5	TPU	NaOH	K_TPU_N
Kevlar	60	13.5 × 13.5	EVA	NaOH	K_EVA_N
Kevlar	60	13.5 × 13.5	TPU	Graphene NP	K_TPU_G
Kevlar	60	13.5 × 13.5	EVA	Graphene NP	K_EVA_G
Kevlar	60	13.5 × 13.5	TPU	NaOH + graphene NP	K_TPU_NG
Kevlar	60	13.5 × 13.5	EVA	NaOH + graphene NP	K_EVA_NG
Kevlar	60	13.5 × 13.5	TPU	(NaOH + silane)	K_TPU_NS
Kevlar	60	13.5 × 13.5	EVA	(NAOH + silane)	K_EVA_NS
Kevlar	60	13.5 × 13.5	TPU	(NaOH + silane) + graphene NP	K_TPU_NSG
Kevlar	60	13.5 × 13.5	EVA	(NaOH + silane) + graphene NP	K_EVA_NSG
UHMWPE	66	15.7 × 11.8	TPU	Control	U_TPU_C
UHMWPE	66	15.7 × 11.8	EVA	Control	U_EVA_C
UHMWPE	66	15.7 × 11.8	TPU	Plasma	U_TPU_P
UHMWPE	66	15.7 × 11.8	EVA	Plasma	U_EVA_P
UHMWPE	66	15.7 × 11.8	TPU	Graphene NP	U_TPU_G
UHMWPE	66	15.7 × 11.8	EVA	Graphene NP	U_EVA_G
UHMWPE	66	15.7 × 11.8	TPU	Plasma + graphene NP	U_TPU_PG
UHMWPE	66	15.7 × 11.8	EVA	Plasma + graphene NP	U_EVA_PG

2.5. Characterization

2.5.1. Yarn Pullout in Laminate Test

The interfacial adhesion between the fibers and matrix was assessed using the yarn pullout in laminate test, with the details of this novel test method outlined in previous work [37,38]. This test evaluates the force required to pull a single yarn from the surrounding matrix, directly measuring yarn–matrix bonding strength.

For each treatment condition, fabric specimens were embedded in the polymer matrix, ensuring that the yarns were well aligned and partially exposed to allow for gripping during the test. The embedded length of the yarns within the matrix was standardized to 20 mm, as seen in Figure 5, to ensure consistency across all specimens. Care was taken to avoid premature damage to the yarns during the embedding process.

The yarn pullout test was conducted using an Instron universal testing machine (34TM-5 with a 5 kN load cell). Each specimen was securely clamped, with the fiber held in the upper grip and the matrix in the lower grip. A constant displacement rate of 0.212 mm/s (0.5 inch/minute) was applied, and the force required to pull the yarn out of the matrix was recorded. The test continued until the yarn was completely separated from the matrix.

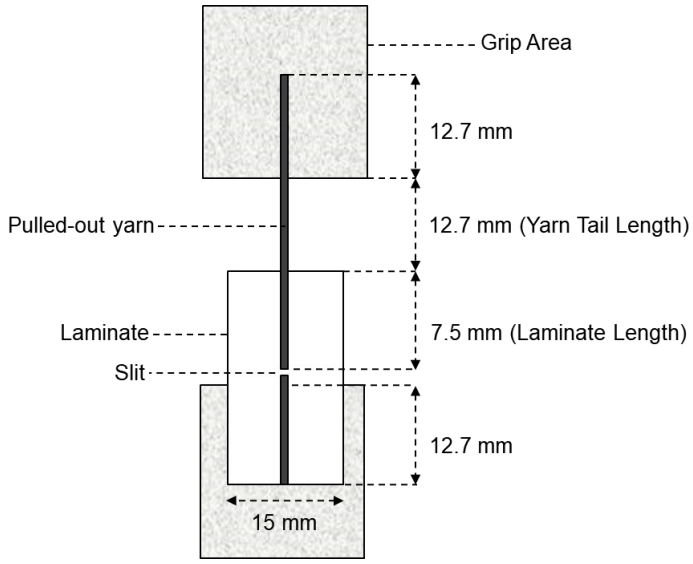


Figure 5. Test panel and specimen for the yarn pullout in laminate test.

We tested at least 10 specimens in each fabric direction for each treatment condition to ensure statistical reliability. Each specimen's peak yarn pullout force (in newtons) was recorded as the measure of adhesion quality between the yarn and the matrix. Both untreated and treated samples were tested, allowing different surface modification techniques to be compared.

The peak yarn pullout force results were averaged for each treatment condition, and standard deviations were calculated to assess variability. Statistical comparisons were made between untreated and treated specimens to evaluate the performance of various surface treatments on enhancing fiber–matrix adhesion. The results were then correlated with the observed surface morphology, particularly concerning the roughness and chemical modifications introduced by the treatments.

2.5.2. Tensile Strength

The tensile strength of the treated and untreated fabric specimens was evaluated using the ASTM D5035-11 [39] (Reapproved 2019) "Standard Test Method for Breaking Force and Elongation of Textile Fabrics (Strip Method)". This method measures a textile fabric's breaking force and elongation by applying a tensile force until the fabric breaks. Rectangular specimens (25 mm × 150 mm) were prepared for each treatment condition, with the long dimension aligned parallel to the warp direction for the warp samples and vice versa for the filling direction of the fabric. The raveled strip method was used for woven fabrics (neat fabrics), where the edges of the specimens were raveled to maintain a consistent width of 25 mm.

The specimens were mounted in a tensile testing machine with smooth, flat jaw faces to prevent slippage or damage during testing. The gauge length between the clamps was set to 75 mm, and the testing speed was fixed at 300 mm/min. The force was applied until the specimen reached its breaking point, and the peak force (in newtons) and elongation (in millimeters) were recorded. Each test was performed on a constant-rate-of-extension tensile testing machine.

Five specimens were tested for the warp direction and eight specimens for the filling direction for each treatment condition, and the average peak force values were reported. The breaking force and elongation results were compared across the different treatment conditions to assess the impact of the surface modifications on the tensile properties of

the fabric. Statistical analysis determined any significant differences between treated and untreated specimens.

2.5.3. Surface Characterization

Fourier transform infrared spectroscopy (FTIR) analysis was performed on the chemically treated Kevlar fibers to identify any chemical changes on the fiber surfaces. FTIR spectra were collected using an FTIR spectrometer equipped with an ATR (Attenuated Total Reflectance) accessory, ensuring direct surface measurement without additional sample preparation. The primary focus was on detecting the presence of new functional groups, such as hydroxyl (OH), carboxyl (COOH), or carbonyl (C=O), that may have been introduced by treatments such as NaOH, silane coupling, and graphene. The chemical changes were compared to understand how each treatment altered the surface chemistry, contributing to improved interfacial adhesion.

Scanning electron microscopy (SEM) was used to visualize the surface morphology of the untreated and treated Kevlar and UHMWPE fibers, providing detailed insight into the topographical changes resulting from various treatments. Samples were sputter-coated with gold to improve conductivity, and images were taken at magnifications ranging from 500× to 5000×. SEM was used to observe the surface roughening caused by the mechanical abrasion and plasma treatments, along with the effects of chemical treatments such as NaOH and silane. The distribution of graphene nanoparticles was also examined to ensure uniform coverage and adequate adhesion to the fiber surfaces. Particular attention was given to identifying features like grooves, fibrillation, and nanoparticle distribution, critical indicators of enhanced surface area and bonding potential with the matrix.

2.5.4. Statistical Analysis

Data collected from the mechanical and adhesion tests, including the tensile strength and yarn pullout tests, were analyzed using one-way analysis of variance (ANOVA) to determine the statistical significance of differences between treatment groups. Before analysis, the data were checked for normality and homogeneity of variances to ensure that the assumptions of ANOVA were met. When necessary, data transformations were applied to satisfy these conditions. Following the ANOVA, a post hoc Tukey test was conducted to identify specific pairwise comparisons between the treatment groups that exhibited significant differences. A significance level of $p < 0.05$ was used for all tests, meaning that any p-value below this threshold was considered statistically significant.

Additionally, the mean values and standard deviations in the form of a bar chart were reported for each treatment group to provide a clear understanding of the variability within the data. The results from the statistical analysis were then interpreted in the context of the observed mechanical performance and surface modifications, allowing for a comprehensive evaluation of how different treatments affected fiber–matrix adhesion.

3. Results and Discussion

3.1. Physical Treatment on Kevlar and UHMWPE: Surface Roughness Study

The goal of the mechanical abrasion was to increase surface roughness to improve the mechanical interlocking between the fibers and the matrix. A Keyence VHX7000 digital microscope visually evaluated the effect of surface roughening on both Kevlar and UHMWPE fibers. In the untreated fabric images shown in Figure 6a,b, the fibers appear smooth and tightly woven with minimal protruding strands. After treatment, the roughened samples show more protruding fibers or "hairs", where the filaments broke, indicating an increase in surface roughness, which can be seen in Figure 6c–e. The untreated samples also have a tighter and more compact weave structure, whereas the treated samples

show slight loosening or separation between the fibers due to the roughening process. This indicates that the one-level roughness treatment substantially increased the average surface roughness for both fiber types. The yarn pullout results in the laminate test are summarized in Figure 7, which shows the mean yarn pullout force for each treatment group. The untreated K_TPU_C samples showed the highest mean pullout force in the group of Kevlar samples. After roughening, the treated K_TPU_T samples displayed a lower mean pullout force with a 9.1% reduction. Similarly, for the K_EVA samples, there was a 26.6% reduction after the roughening treatment. In contrast to Kevlar, the UHMWPE samples showed a substantial improvement after treatment. U_TPU samples showed a 90.4% increase post-treatment, while U_EVA showed a 29.9% increase.

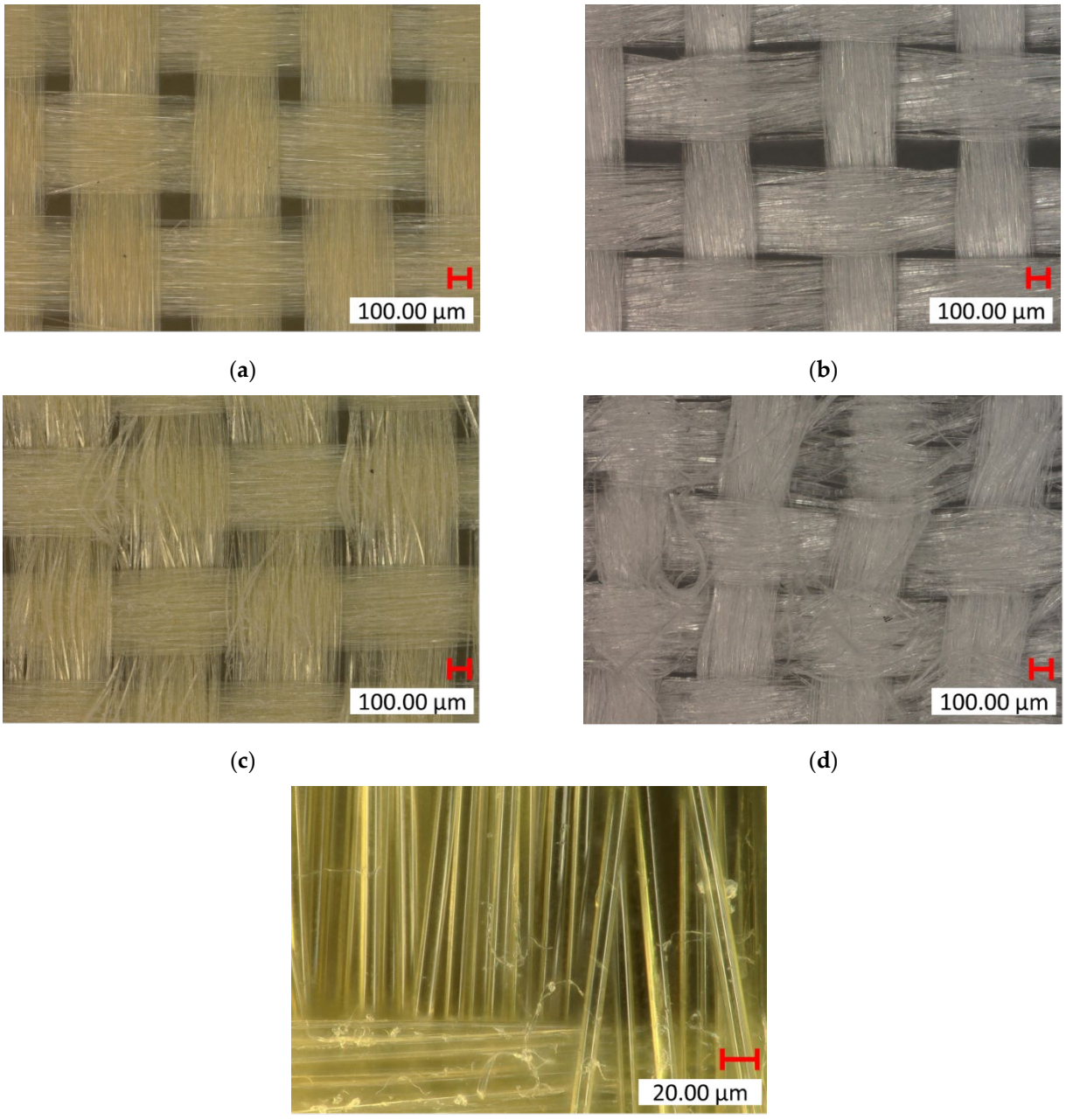


Figure 6. Digital microscopic (Keyence VHX7000) images of fabric samples. Control: (**a**) Kevlar (×100 mag.) and (**b**) UHMWPE (×100 mag.). Post-treatment: (**c**) Kevlar (×100 mag.), (**d**) UHMWPE (×100 mag.), and (**e**) Kevlar (×1000 mag.).

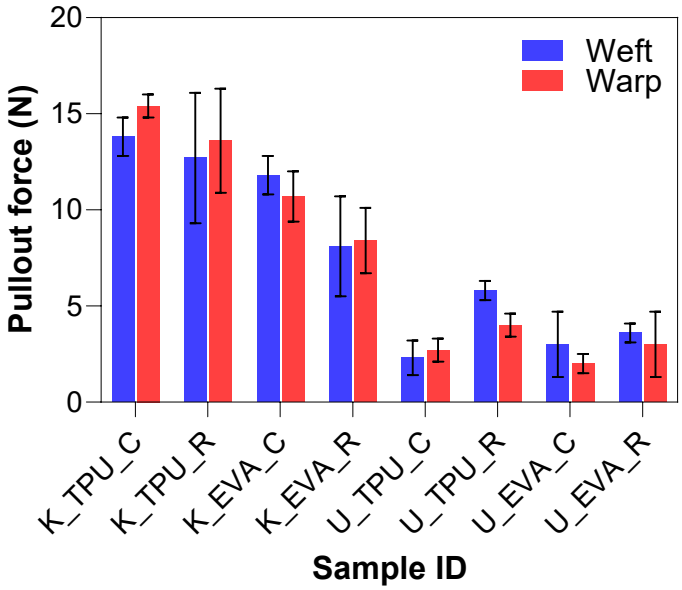


Figure 7. Yarn pullout in laminate test results for physically treated samples.

Surface abrasion treatment effectively works for UHMWPE because it introduces surface roughness, which enhances adhesion. This effect is tied to UHMWPE's inherently smooth and chemically inert surface, which gains bonding sites through abrasion [3]. In contrast, Kevlar's structure is more chemically reactive, making surface abrasion less impactful. The difference in the impact of surface abrasion between UHMWPE and Kevlar may also be attributed to these fibers' inherent structural and chemical properties. UHMWPE, semi-crystalline in nature, comprises long, linear molecular chains with relatively low intermolecular forces, making it more susceptible to physical changes from friction-based treatments. When subjected to surface abrasion, the outer layers of UHMWPE fibers experience increased roughness, which enhances mechanical interlocking with the matrix. In contrast, Kevlar is known for its highly crystalline and ordered structure, with strong intermolecular hydrogen bonds contributing to its high thermal and chemical resistance. This crystalline structure may cause Kevlar to be less responsive to friction-based treatments like abrasion, as the surface remains relatively smooth despite the treatment. As a result, the mechanical interlocking achieved through abrasion is less effective in Kevlar than in UHMWPE.

Additionally, their structural configurations can further explain the difference in surface abrasion performance between the UHMWPE and Kevlar fabrics. Despite having analogous areal densities, the fabric counts for the two materials varied significantly. UHMWPE has a fabric count of 15.7 by 11.8 ends/cm, while Kevlar was a more compact square weave with 13.5 by 13.5 ends/cm. This difference in fabric count means that UHMWPE fibers had more room to move within the weave, allowing for greater loosening and separation of fibers or filaments during roughening. This separation created additional pathways for the matrix material to penetrate deeper into the fabric, enhancing mechanical interlocking and improving adhesion. In contrast, the tighter and more compact weave of Kevlar restricted the space available for fiber movement and matrix penetration. As a result, the roughening process was less effective in creating surface texture that would allow for enhanced interlocking and adhesion. Kevlar's inherent compactness and high crystallinity further limited the changes that could be achieved through mechanical abrasion, reinforcing its resistance to surface modification. These factors collectively illustrate why UHMWPE responded better to physical roughening treatments, improving adhesion, while Kevlar remained resistant due to its compact weave and high structural rigidity.

The Tukey–Kramer analysis was conducted to compare the mean pullout forces for different treatments, and the results are summarized by connecting letters in Table 3. Treatments with the same letter designation indicate no significant difference between them, while different letters represent statistically significant differences. The analysis revealed that K_TPU_C (Group A) and K_TPU_R (Group A) are not significantly different, showing that the TPU-treated and untreated Kevlar laminates have similar pullout forces, with the untreated TPU slightly outperforming the treated. K_EVA_C (Group B) is significantly lower than the TPU-treated groups but still higher than the treated and untreated EVA and UHMWPE laminates. The treated K_EVA_R (Group C) was significantly different from all other Kevlar treatments, indicating a reduction in pullout force after treatment. For UHMWPE, the treated U_TPU_T (Group D) and U_EVA_R (Group D/E) laminates demonstrated a significant increase in pullout force compared to their untreated counterparts, although they still showed lower values than Kevlar laminates. Finally, the untreated U_TPU_C (Group E) and U_EVA_C (Group E) exhibited the lowest pullout forces, with no significant difference between the TPU and EVA matrices. Overall, the results indicate that Kevlar/TPU laminates have the highest adhesion, while UHMWPE laminates, despite improvements after treatment, remain significantly weaker in comparison.

Table 3. Tukey–Kramer analysis results for mean pullout forces.

Level					
K_TPU_C	A				
K_TPU_R	A				
K_EVA_C		B			
K_EVA_R			C		
U_TPU_R				D	
U_EVA_R				D	E
U_TPU_C					E
U_EVA_C					E

In contrast to Kevlar, where surface treatments resulted in reductions in pullout force, this study found that UHMWPE exhibited increased adhesion strength after treatment. However, while the improvements for UHMWPE were statistically significant, the absolute values of pullout force remained relatively low compared to Kevlar, even after treatment. This limitation stems from the inherent characteristics of UHMWPE fibers, which lack functional groups such as hydroxyl or amide groups that would otherwise allow for stronger chemical bonding with the matrix. As a result, the effectiveness of surface treatments like roughening is still limited by the fiber's chemical inertness. In practical applications, this means that while the increase in surface roughness can enhance the interfacial adhesion of UHMWPE, the increases may still not be sufficient for high-performance or load-bearing uses, especially when compared to Kevlar, which has a higher baseline adhesion due to its hydrogen bonding capability. The lack of functional groups in UHMWPE limits its ability to form strong chemical bonds with the matrix, making it less suitable for applications requiring high adhesion strength, even after this abrasion treatment.

The tensile test results provided insights into the mechanical performance of Kevlar and UHMWPE fiber-reinforced laminates treated with physical roughening and tested in both the warp and weft directions. The summary can be seen in Figure 8. There were no significant differences in tensile strength for the Kevlar samples. However, the UHMWPE laminates displayed notably different behavior from Kevlar, particularly in the weft direction. The untreated U_EVA_C group exhibited a high mean tensile strength of 852.17 N, with a standard deviation of 104.31 N, indicating good overall strength and consistency. In contrast, after roughening, the treated U_EVA_R group drastically reduced

its tensile strength to 382.38 N, representing a 55.2% decrease. Similarly, there was a 45.7% reduction in strength for the U_TPU samples.

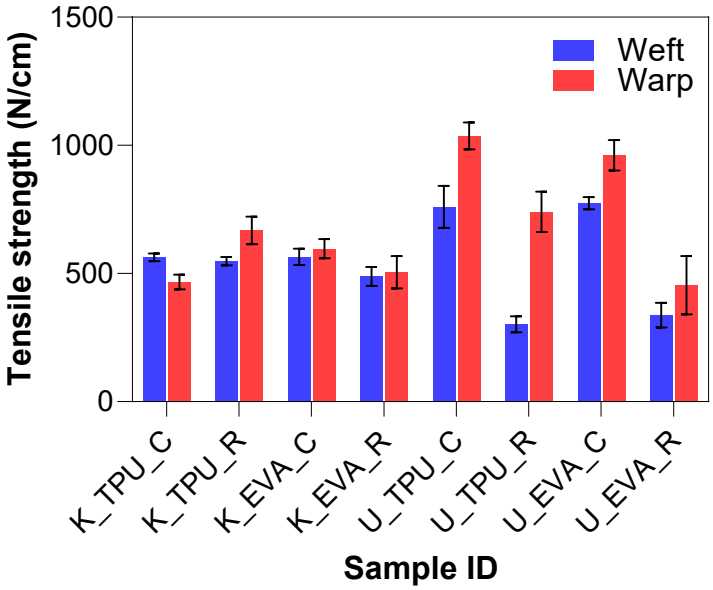


Figure 8. Tensile strength results for physically treated samples.

The significant drop in tensile strength after roughening can be attributed to the breakage of some filaments during the abrasion process, as illustrated in Figure 6e, and the misalignment of those that remained intact. The roughening treatment can cause individual filaments to shift from their original straight orientation. This misalignment reduces their effective contribution to the overall tensile strength. When filaments are tilted, their contribution to the tensile load becomes a function of the cosine of the angle relative to the applied force. In other words, if a filament is perfectly aligned with the load (angle of zero degrees), its full breaking load is realized. However, as the angle increases due to misalignment, the effective strength of each filament is reduced by the cosine of that angle. This combined effect of filament breakage and misalignment reduces the tensile strength of UHMWPE laminates, limiting the practical applicability of physical roughening, particularly in load-bearing applications.

3.2. Chemical Treatments on UHMWPE

To address the inherent limitations of UHMWPE's lack of functional groups, plasma treatment was investigated as an alternative approach to improve interfacial adhesion by introducing reactive sites on the otherwise inert fiber surface. Fourier transform infrared spectroscopy (FTIR) spectra (Figure 9) provided insights into the chemical bonds and surface functionalities of the UHMWPE samples. In all samples, characteristic peaks of UHMWPE were observed around 2916 cm^{-1} and 2847 cm^{-1}, corresponding to CH_2 asymmetric and symmetric stretching vibrations, respectively. These peaks are a hallmark of the polymer backbone in UHMWPE, indicating the integrity of the polyethylene chains. The spectrum displayed only these characteristic peaks for the control sample (U_C), signifying a relatively unmodified UHMWPE structure. The FTIR analysis for the untreated UHMWPE (U_C) revealed additional peaks that diverge from the spectra typically reported in the literature for pure UHMWPE. These extra peaks could indicate external substances, such as impurities or added stabilizers like UV blockers. Considering these samples were sourced from external suppliers, the unexpected peaks may be attributed to processing agents or functional additives incorporated during commercial production. To further validate these observations, subsequent investigations will use laboratory-grade, pure

UHMWPE to eliminate uncertainties regarding external influences. The analysis of Kevlar samples revealed similar additional peaks, so further studies using pure Kevlar samples will also be conducted to confirm these observations.

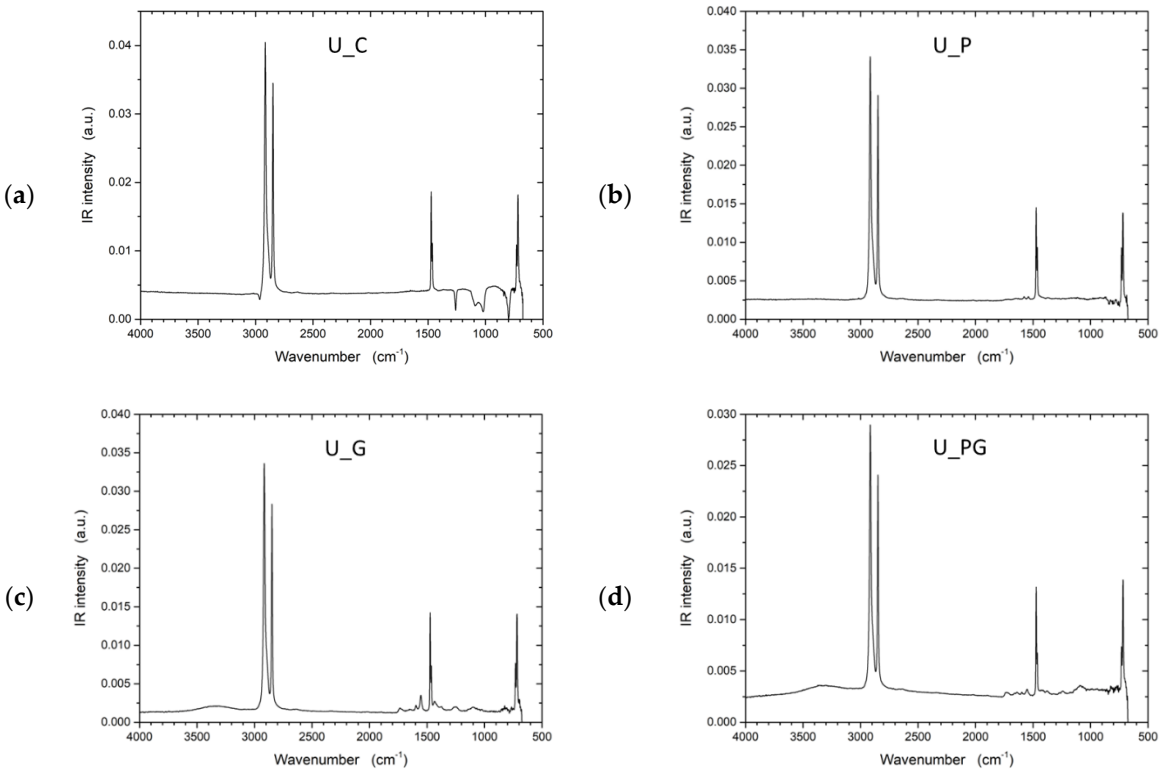


Figure 9. FTIR spectra of untreated UHMWPE and treated UHMWPE samples: (**a**) control, (**b**) plasma treated, (**c**) graphene NP treated, and (**d**) plasma and graphene NP treated.

The FTIR spectrum exhibited notable changes in the plasma-treated sample (U_P). The intensity of CH_2 peaks slightly decreased, indicating possible chain scission or cross-linking induced by plasma exposure. Additionally, new peaks around 3400–3500 cm^{-1} were evident, suggesting the formation of hydroxyl groups (-OH) due to oxidation processes. The FTIR spectrum of the U_G sample shows characteristic peaks for UHMWPE, including the strong –CH_2- stretching vibrations at 2916 cm^{-1} and 2847 cm^{-1}, indicating the polymer backbone remains intact. New peaks near 1500–1800 cm^{-1} suggest C=C bonds from the incorporated graphene, and a small peak around 1730 cm^{-1} indicates possible carbonyl groups from minor oxidation or residual functional groups on the graphene. Broadening around 1000–1200 cm^{-1} suggests C–O bonds, hinting at interactions between graphene and the polymer matrix. The combined graphene and plasma-treated sample (U_PG) showed a mix of characteristics from both individual treatments. Peaks indicating C=C bonds from graphene were visible alongside the peaks corresponding to oxidation effects caused by plasma treatment.

Raman spectroscopy (Figure 10) provided complementary information on the structural modifications within the samples, focusing on molecular vibrations and lattice changes. The untreated UHMWPE (U_C) sample exhibited a typical Raman spectrum for polyethylene, with the most prominent peaks arising from CH_2 bending and stretching vibrations, indicating the polymer's structural integrity. The graphene-treated sample (U_G) displayed significant changes in the Raman spectrum, with the appearance of peaks around 1350 cm^{-1} (D band) and 1580 cm^{-1} (G band). These peaks indicate the presence of graphene, where the D band suggests the introduction of disorder or defects, and the G

band reflects the in-plane vibration of sp^2-bonded carbon atoms. The emergence of these peaks confirmed the successful incorporation of graphene on the UHMWPE surface.

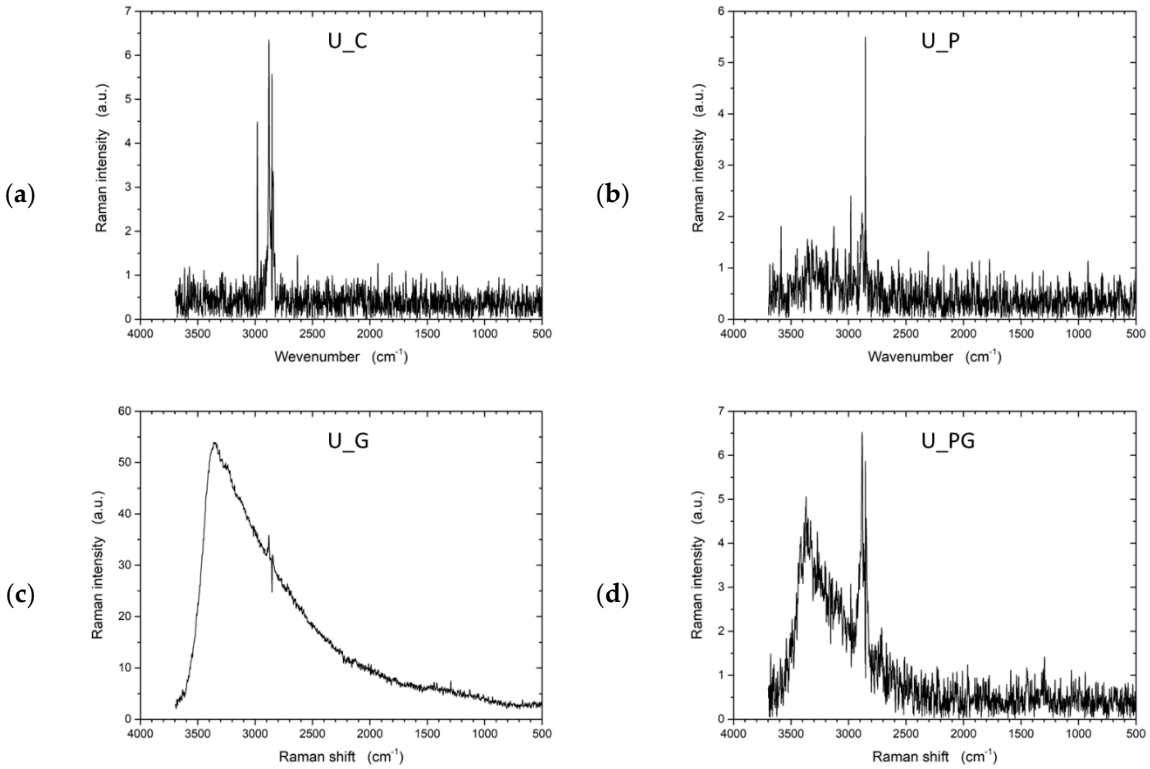


Figure 10. Raman spectra of untreated UHMWPE and treated UHMWPE samples: (**a**) control, (**b**) plasma treated, (**c**) graphene NP treated, and (**d**) plasma and graphene NP treated.

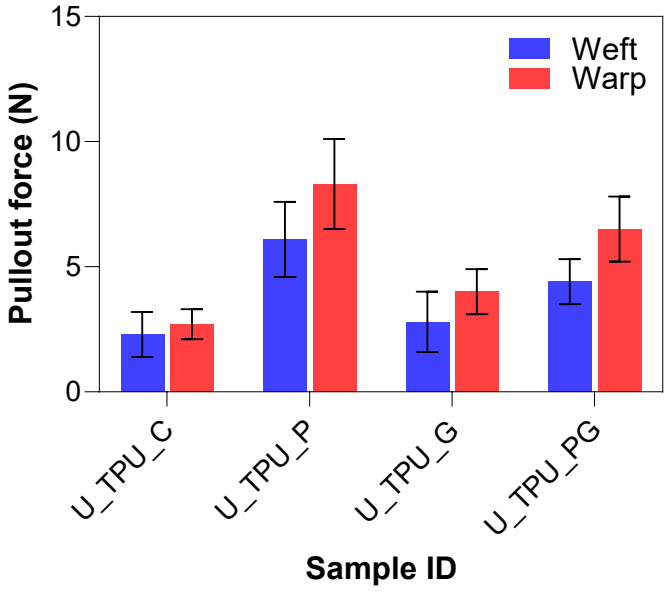
For the plasma-treated sample (U_P), the Raman spectrum revealed a more amorphous structure than the untreated sample. The decrease in intensity and broadening of characteristic peaks indicate structural modifications such as chain scission or cross-linking caused by plasma exposure. Plasma treatment often leads to the formation of amorphous carbon regions, which can be observed as a broadening of the peaks in the Raman spectrum. In the combined graphene and plasma-treated sample (U_PG), the Raman spectrum showed both the D and G bands associated with graphene and evidence of amorphous carbon regions.

The pullout force results for the plasma and graphene treatments on UHMWPE FRLs are summarized in Figure 11. The results of the surface treatments on UHMWPE samples demonstrate significant variations in yarn pullout force depending on the type of treatment applied and the matrix material (EVA or TPU). The untreated control samples showed the lowest yarn pullout forces, while plasma and graphene treatments, both individually and in combination, led to notable increases in interfacial adhesion. The untreated control samples for both EVA and TPU matrices exhibited similar poor yarn pullout forces, which showed that UHMWPE fibers have poor adhesion to both matrices, primarily due to their chemically inert nature and lack of functional groups that facilitate bonding.

The plasma-treated samples significantly improved yarn pullout force, particularly with the TPU matrix. The U_EVA_P samples had a 106.2% increase, indicating that plasma treatment effectively roughened the fiber surface and introduced reactive sites that facilitated better bonding with the EVA matrix. FTIR analysis confirmed the formation of hydroxyl groups (-OH) around 3400–3500 cm^{-1} and a slight reduction in the CH_2 peak intensity, indicating surface oxidation and chain scission, which likely enhanced chemical bonding with the EVA matrix. The UP_TPU samples exhibited an even more pronounced

improvement, with a percent increase of 188.1%, nearly triple that of the control samples. The superior performance of the TPU matrix in combination with plasma treatment suggests that TPU has a stronger affinity for the modified surface of UHMWPE possibly due to amorphous carbon regions from plasma treatment confirmed by the Raman analysis, allowing for better mechanical interlocking and bonding with TPU. The addition of graphene nanoparticles (UG) led to a moderate improvement in yarn pullout force. The UG samples showed a slightly higher increase in yarn pullout force than the control samples. U_EVA_G had a 56.5% increase, while U_TPU_G had a 35.2% increase. FTIR and Raman spectra indicated the successful incorporation of graphene, with C=C and C–O bonds enhancing surface functionality. However, the overall effect was limited by UHMWPE's smooth surface and lack of bonding sites. While graphene nanoparticles introduced some surface functionalization that enhanced adhesion, the overall effect was limited. This suggests that while graphene helps, it does not fully overcome the bonding challenges of UHMWPE, likely due to the fiber's smooth surface and lack of natural bonding sites.

(**a**)



(**b**)

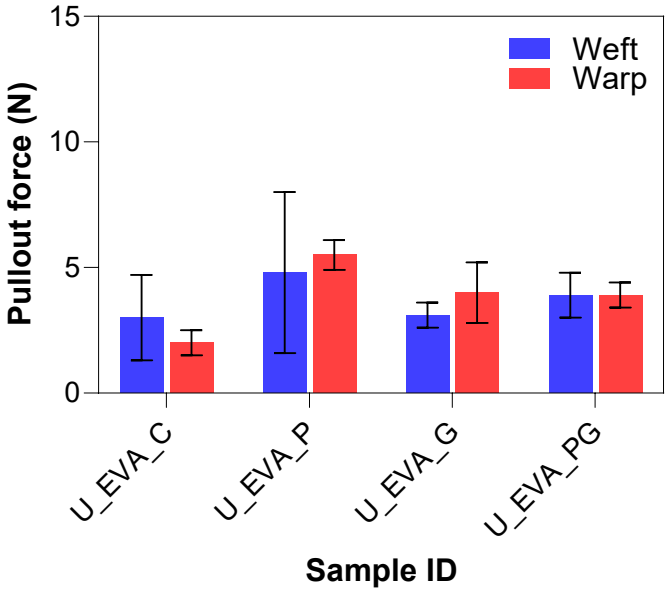


Figure 11. Yarn pullout in laminate test results of UHMWPE laminates with (**a**) TPU matrix and (**b**) EVA matrix.

The combination of plasma and graphene (PG) offered mixed results. In the U_EVA_PG samples, the yarn pullout force had a 56.5% increase, higher than the graphene-only treatment but still lower than the plasma-only treatment. This indicates that while the combination of plasma and graphene improves adhesion compared to the control, it does not outperform plasma treatment alone in the EVA matrix. For the U_TPU_PG samples, the yarn pullout force increased by 118.8%, which is again higher than the control and graphene-treated samples but still lower than the plasma-only treatment. The combination of plasma and graphene may have introduced additional functional groups, but the overall improvement was not as substantial as plasma treatment alone. The lower performance of the combined plasma and graphene (PG) treatment, particularly compared to the plasma-only treatment, can be attributed to the fact that the graphene application was a wet treatment. This wet process may have partially washed away some of the surface functionalization introduced by the plasma treatment. Plasma roughening created reactive sites and functional groups, but the subsequent wet graphene coating could have diminished these effects by washing off the functional groups, thereby reducing the overall interfacial adhesion. To mitigate the issue of graphene washing away plasma-induced functional groups, a potential strategy could involve applying graphene prior to plasma treatment, allowing the plasma process to stabilize the graphene coating while simultaneously introducing additional surface functionalization. Additionally, optimizing plasma parameters, such as treatment duration and energy levels, could help preserve the functionalized surface and enhance the overall performance of the combined treatment. The Tukey analysis in Table 4 further confirms that plasma-treated samples had the highest yarn pullout forces, indicating superior adhesion to other treatments. Plasma plus graphene treatments were statistically lower, likely due to the wet graphene application reducing the plasma's surface effects. Graphene-only had the lowest improvement to the control samples.

Table 4. Tukey–Kramer analysis of yarn pullout forces for UHMWPE laminates.

Level				
U_TPU_P	A			
U_TPU_PG		B		
U_EVA_P		B		
U_EVA_PG			C	
U_EVA_G			C	
U_TPU_G			C	
U_TPU_C				D
U_EVA_C				D

These results suggest that while plasma treatment induces surface roughness, the primary contribution to adhesion improvement comes from the chemical functionalization of the fiber surfaces. For UHMWPE, which lacks reactive sites, plasma treatment proved effective in introducing functional groups that facilitated stronger matrix bonding. The tensile test results, as indicated by the Tukey–Kramer HSD analysis (Table 5), showed that the treatments applied to the UHMWPE samples had varied effects on their tensile properties, with some treatments resulting in noticeable reductions in performance across both EVA and TPU matrices. For TPU-based samples, the U_TPU_P treatment resulted in a 5.04% increase in weft performance and a negligible 0.81% decrease in warp strength, suggesting a limited impact of plasma treatment on tensile properties. The U_TPU_G treatment showed a 7.75% decrease in weft performance and a more noticeable 23.91% reduction in warp strength, indicating that the addition of graphene had an adverse effect on tensile properties. The combined treatment (U_TPU_PG) exhibited a marginal 0.87% increase in weft performance, but warp strength decreased by 16.14%, showing that

the combined effect of plasma and graphene was also not significantly beneficial to the tensile strength.

Table 5. Tukey–Kramer analysis of tensile strength for UHMWPE laminates.

Level		
U_TPU_P	A	
U_TPU_C	A	
U_EVA_C	A	B
U_EVA_PG	A	B
U_EVA_P	A	B
U_EVA_G	A	B
U_TPU_PG	A	B
U_TPU_G		B

For EVA-based samples, the U_EVA_P treatment led to a slight 0.79% decrease in weft performance and a 9.22% reduction in warp strength. Similarly, the U_EVA_G treatment resulted in a 3.70% decrease in weft performance and a 5.86% reduction in warp strength. The combined treatment (U_EVA_PG) showed a 3.58% decrease in weft performance and a minimal 0.41% reduction in warp strength, suggesting that the combined plasma and graphene treatment had no substantial effect on tensile properties for the EVA matrix. The tensile test results, as indicated by the Tukey–Kramer HSD analysis (Table 5), showed that the treatments applied to the UHMWPE samples had varied effects on their tensile properties, with a general trend of strength reduction. However, no consistent trend was observed across treatments. The differences between the TPU and EVA matrices, where EVA showed minimal reductions compared to TPU, suggest that the observed variation may be attributed to other factors, such as natural variability. Since the adhesive layer does not contribute to the tensile strength of the material, its presence or modification should not significantly affect the tensile properties of the material.

The plasma-treated TPU samples (U_TPU_P) exhibited the highest tensile strength, placing them in group "A", alongside the untreated TPU and EVA controls (U_TPU_C and U_EVA_C), which also showed high tensile strength with no significant differences. The plasma-only EVA samples (U_EVA_P) and the plasma plus graphene-treated samples (UPG_EVA, UPG_TPU) remained within the same group (A/B), indicating that the treatments did not significantly affect the tensile properties. The bar chart summary can be seen in Figure 12.

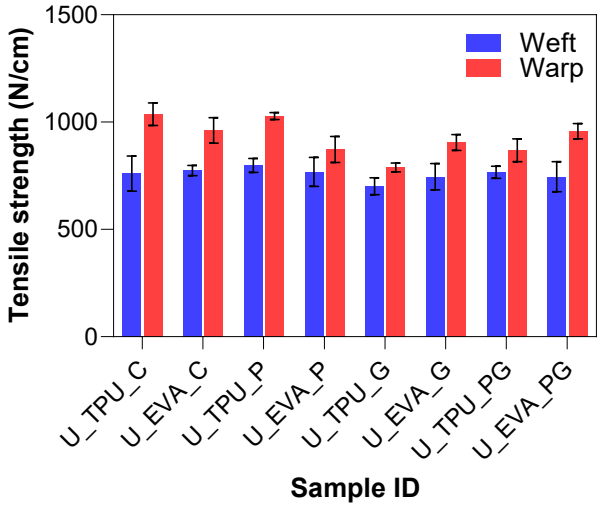


Figure 12. Tensile strength results of UHMWPE laminates.

3.3. Chemical Treatments on Kevlar Fibers

The FTIR spectrum of the Kevlar samples before and after the various treatments were also collected. They are plotted in Figure 13. The untreated Kevlar (K_C) exhibited characteristic peaks typical of polyaramid structures. Notable peaks included the N–H stretching vibration around 3300 cm^{-1}, indicative of strong hydrogen bonding within the polymer, and the amide I band (C=O stretching) at 1650 cm^{-1}, along with the amide II band (N–H bending) at 1530 cm^{-1}. These peaks are common in Kevlar due to its aromatic content and amide linkages. For the graphene-treated sample (K_G), additional peaks in the 1050–1100 cm^{-1} range were observed, corresponding to C–O–C vibrations, suggesting an interaction between the Kevlar surface and graphene nanoparticles. A new peak at around 1710 cm^{-1} could indicate the formation of C=O groups, possibly due to graphene's oxidative effects or interactions between the polymer matrix and graphene particles. In the NaOH-treated sample (K_N), the characteristic peaks of Kevlar shifted slightly, indicating minor changes in hydrogen bonding and amide structures. These shifts are likely due to partial hydrolysis or surface etching induced by the alkaline treatment. In the sample treated with NaOH and graphene nanoparticles (K_NG), the FTIR spectrum showed peaks similar to the K_G sample, adding a more defined C=O peak around 1710 cm^{-1}. This suggests that the combination of NaOH treatment and graphene nanoparticle addition led to stronger interactions and enhanced oxidation on the Kevlar surface. The NaOH and silane-treated Kevlar sample (K_NS) exhibited new peaks around 1100–1150 cm^{-1}, attributed to Si–O stretching vibrations, indicating successful silane grafting. These changes suggest increased chemical functionality on the Kevlar surface. In the NaOH, silane, and graphene-treated sample (K_NSG), additional peaks appeared around 1050 cm^{-1} and 1740 cm^{-1}, corresponding to C–O–C and C=O stretching vibrations, respectively. These observations confirm the successful incorporation of silane and graphene functionalities, leading to a more chemically functionalized surface.

Figure 14 shows the Raman spectroscopy results of the various Kevlar treatments. The Raman spectrum of the control sample (K_C) (Figure 14a) displayed characteristic peaks associated with Kevlar's aromatic backbone. The D band at around 1340 cm^{-1} and the G band at approximately 1580 cm^{-1} are typical for Kevlar and indicate its aromatic structure and graphitic-like properties. In the graphene-treated sample (K_G), the G band became more pronounced, indicating the successful addition of graphene nanoparticles. The relative intensity of the D band also increased, pointing to the introduction of structural defects or disruptions in the aromatic structure caused by graphene incorporation. For the NaOH-treated sample (K_N), the D and G bands remained relatively stable with minor shifts, suggesting some structural changes or oxidation of the aromatic rings induced by the alkaline treatment.

In the sample treated with NaOH and graphene nanoparticles (K_NG), the G band around 1580 cm^{-1} was more intense, indicating increased graphene content. The intensified D band suggested that the combined treatment introduced increased defects. The NaOH and silane-treated sample (K_NS) displayed new peaks associated with Si–O interactions, confirming successful silane grafting. The Raman spectrum showed these new features without significantly altering the primary Kevlar vibrations, indicating that silane treatment primarily affected surface functionalities. Lastly, in the NaOH, silane, and graphene-treated sample (K_NSG), the Raman spectrum exhibited a strong G band at around 1580 cm^{-1} and an intensified D band at around 1340 cm^{-1}, suggesting the successful integration of both silane and graphene functionalities. This indicates a well-modified Kevlar surface with enhanced chemical interactions.

Figure 15a,b summarize the yarn pullout in laminate test results for the different treatment methods on the Kevlar FRLs. The yarn pullout test of the Kevlar treatment

study demonstrated notable differences in adhesion performance across various surface modifications and matrix materials (EVA and TPU). Overall, the treatments applied to the Kevlar fibers significantly impacted their interfacial adhesion, with the combination of sodium hydroxide, silane, and graphene (NSG) yielding the highest performance in both matrices. For Kevlar/EVA laminates, the untreated control samples (K_EVA_C) had a mean yarn pullout force of 11.26 N, which served as a baseline for comparison. The introduction of surface treatments generally improved the adhesion strength. Graphene-only (K_EVA_G) increased the mean yarn pullout force by 8.2%, showing a modest improvement over the control due to the added surface functionalization from graphene nanoparticles. NaOH-only (K_EVA_N) also resulted in a slight percentage increase of 3.6%, suggesting that the alkaline treatment helped introduce functional groups to the surface. However, the effect was not as pronounced as with other treatments.

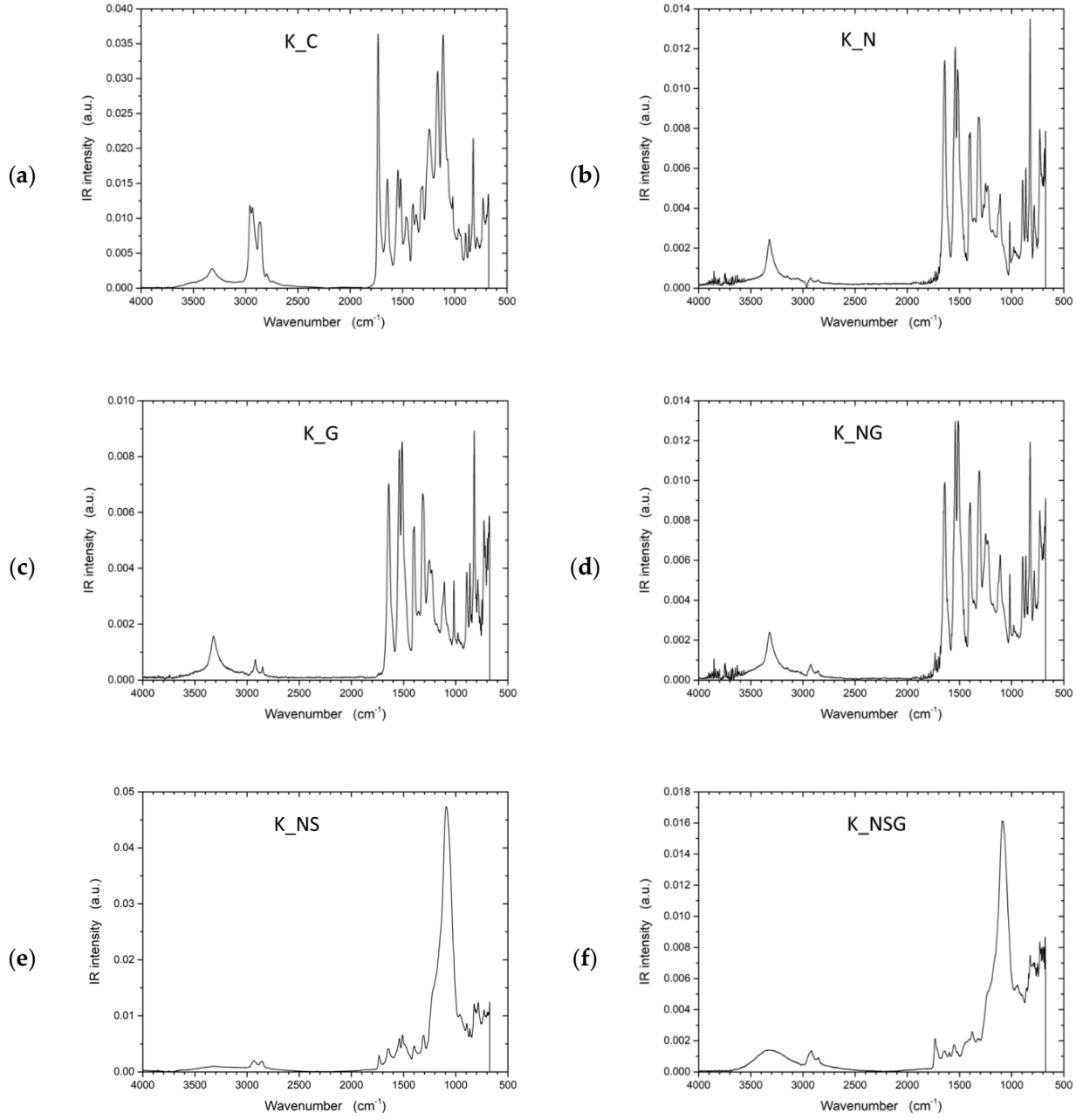


Figure 13. FTIR spectra of untreated Kevlar and treated Kevlar samples: (**a**) control, (**b**) NaOH treated, (**c**) graphene NP treated, (**d**) NaOH and graphene NP treated, (**e**) NAOH and silane treated, and (**f**) NAOH, silane, and graphene NP treated.

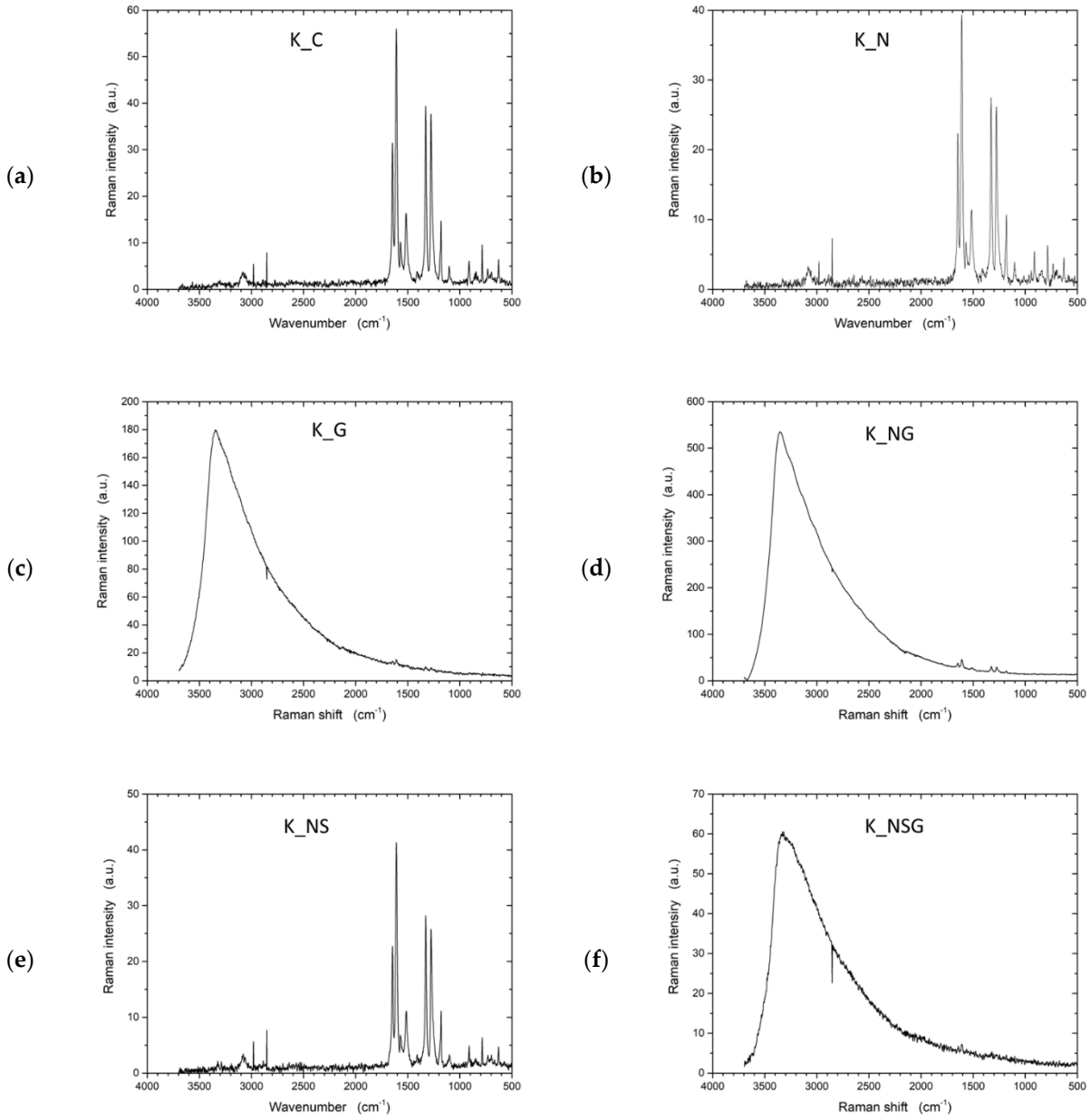


Figure 14. Raman spectra of untreated Kevlar and treated Kevlar samples: (**a**) control, (**b**) NaOH treated, (**c**) graphene NP treated, (**d**) NaOH and graphene NP treated, (**e**) NAOH and silane treated, and (**f**) NAOH, silane, and graphene NP treated.

The combination of NaOH and graphene (K_EVA_NG) further improved adhesion by 9.2%, showing that combining treatments enhanced bonding with the EVA matrix. NaOH and silane (K_EVA_NS) increased adhesion by 11.9%, indicating that silane acted effectively as a coupling agent to enhance fiber–matrix bonding. The most significant improvement was seen in the combined NaOH, silane, and graphene (K_EVA_NSG) treatment, where the mean yarn pullout force increased considerably by 95.4%, almost double the adhesion strength compared to the other treatments. This suggests that the synergistic effect of all three treatments (alkaline, silane, and graphene) produced optimal surface functionalization and mechanical interlocking.

For Kevlar/TPU laminates, the untreated control samples (K_TPU_C) showed a higher baseline yarn pullout force of 14.47 N than the EVA matrix. Graphene-only (K_TPU_G) led to a moderate increase of 9.7%, slightly higher than in the EVA matrix, indicating that graphene had a stronger effect when used with TPU. The NaOH-only (K_TPU_N) treatment

did not perform as well as expected, with a mean yarn pullout force lower than the control, resulting in an 18.5% decrease suggesting that the TPU matrix may not have interacted well with the NaOH treatment alone. However, NaOH and graphene (K_TPU_NG) significantly boosted the adhesion strength by 21.7%, indicating that combining treatments enhanced bonding with TPU. The NaOH and silane (K_TPU_NS) treatment further improved the yarn pullout force by 32.6%, demonstrating that silane worked well with TPU to improve fiber–matrix interaction. The most effective treatment was again the combination of NaOH, silane, and graphene (K_TPU_NSG), representing a 76.6% increase in adhesion strength. This highlights the impact of combining these treatments to maximize surface modification and bonding strength with TPU.

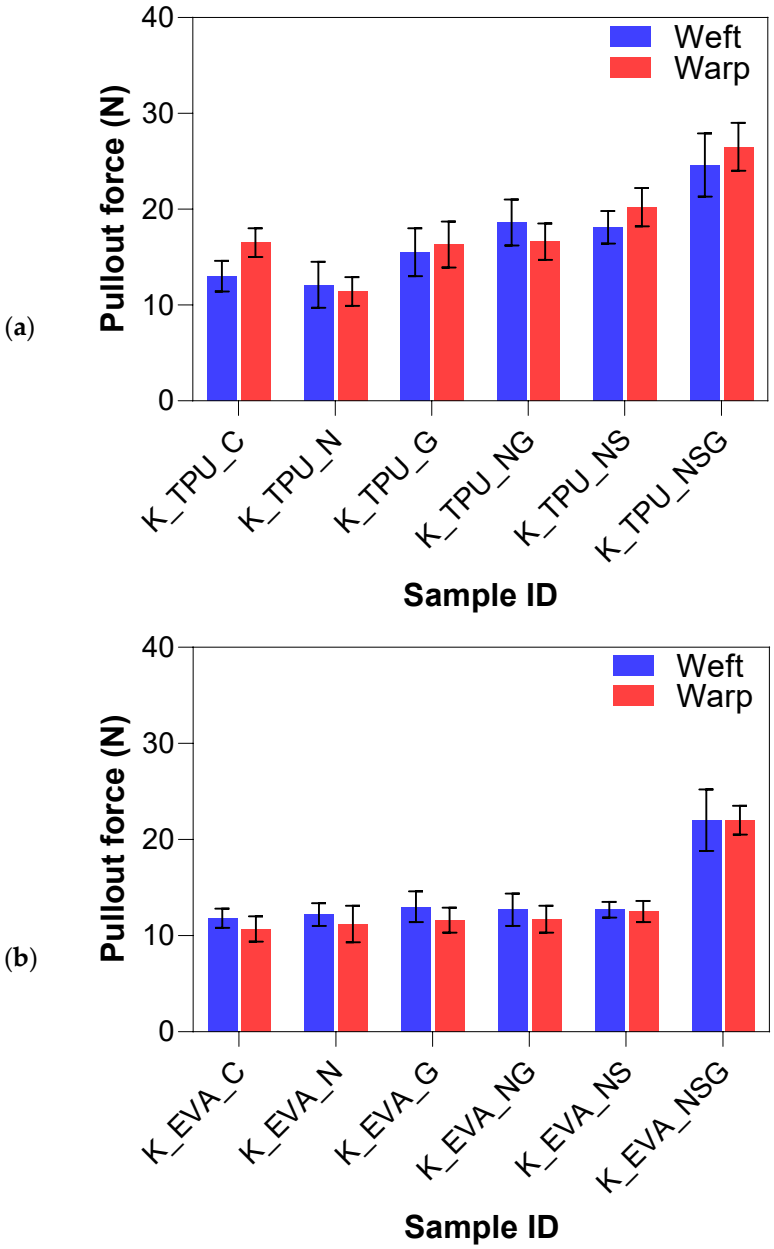


Figure 15. Yarn pullout in laminate test results of Kevlar laminates with (**a**) TPU matrix and (**b**) EVA matrix.

The Tukey–Kramer analysis in Table 6 further highlights that Kevlar laminates with NaOH, silane, and graphene treatment (NSG) in the TPU matrix achieved the highest pullout forces (Group A), indicating the strongest interfacial adhesion. The same NSG treatment in EVA (Group B) also showed strong adhesion but was slightly less effective

than in TPU. The NaOH + silane (NS) and NaOH + graphene (NG) treatments in TPU (Groups C/D) were effective but not as strong as NSG. Graphene-only treatment (Group D/E) provided modest improvements, while untreated controls and single treatments in EVA (Groups F/G) showed the lowest adhesion levels. This analysis confirms that combined chemical treatments, especially NSG, significantly enhance fiber–matrix bonding, with TPU proving to be the more effective matrix.

Table 6. Tukey–Kramer analysis of yarn pullout forces for Kevlar laminates.

Level							
K_TPU_NSG	A						
K_EVA_NSG		B					
K_TPU_NS			C				
K_TPU_NG			C	D			
K_TPU_G				D	E		
K_TPU_C					E	F	
K_EVA_NS						F	G
K_EVA_NG						F	G
K_EVA_G						F	G
K_TPU_N							G
K_EVA_N							G
K_EVA_C							G

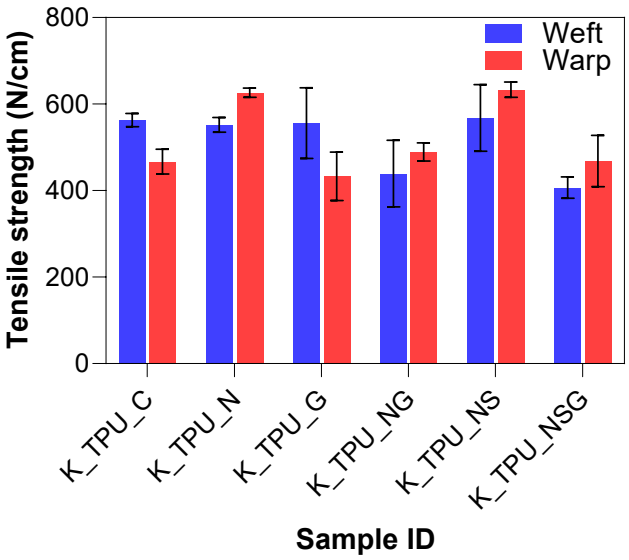
The tensile results (Figure 16) show nuanced differences across the treatments applied to Kevlar-reinforced laminates, with some treatments offering slight improvements while others had detrimental effects. Most of the samples stayed in the same range except for minor variations. For TPU-based samples, the N_TPU treatment showed a minor reduction in weft performance (1.95% decrease) but a significant improvement in warp performance (34.12% increase), indicating that the treatment may enhance structural integrity along the warp direction. The G_TPU treatment resulted in a negligible reduction in weft performance (1.23% decrease) and a slight reduction in warp performance (7.26% decrease), suggesting that graphene application had minimal benefit for tensile properties in the TPU matrix. Conversely, the NG_TPU treatment showed a notable reduction in weft performance (21.99% decrease) but a small improvement in warp performance (4.80% increase), while the NS_TPU treatment led to a minimal increase in weft performance (0.87% increase) and a significant improvement in warp performance (35.64% increase). Finally, the combined NSG_TPU treatment demonstrated the largest reduction in weft performance (27.74% decrease) but maintained warp performance with a negligible change (0.32% increase). For EVA-based samples, the N_EVA treatment caused a moderate decrease in weft performance (5.86% decrease) and a slight improvement in warp performance (1.19% increase), indicating minimal impact on overall tensile strength. The G_EVA treatment showed a notable increase in weft performance (9.56% increase) but a significant reduction in warp performance (32.34% decrease), highlighting a contrasting effect of graphene in the EVA matrix compared to TPU. The NG_EVA treatment led to a substantial improvement in weft performance (22.64% increase) but a moderate reduction in warp performance (11.45% decrease). In contrast, the NS_EVA treatment resulted in a small reduction in both weft (2.08% decrease) and warp performance (10.09% decrease), suggesting limited effectiveness. Lastly, the combined NSG_EVA treatment exhibited the largest reduction in weft performance (33.22% decrease) and a significant reduction in warp performance (24.64% decrease), suggesting that the combination of treatments may have weakened the overall structure.

Overall, the results indicate that the impact of treatments on Kevlar tensile properties varied significantly depending on the matrix and direction (warp or weft). While some

treatments showed potential for improving warp performance (e.g., N_TPU with a 34.12% increase and NS_TPU with a 35.64% increase), others resulted in substantial reductions, particularly in weft performance, or demonstrated no consistent trend. Among the treatments, the NaOH, silane, and graphene (NSG) treatment showed the most consistent trend of reduction across both matrices. In the EVA matrix, NSG resulted in a 33.22% decrease in weft performance and a 24.64% decrease in warp performance, while in the TPU matrix, it caused a 27.74% decrease in weft performance and a minimal 0.32% increase in warp performance. This suggests that over-modification of the fiber surface, particularly when combining multiple treatments, can weaken its mechanical properties due to fiber degradation from too many treatments.

The Tukey–Kramer analysis (Table 7) reflects these subtle differences. Although five distinct groups were identified, most treatments appear in multiple groups, indicating that the tensile properties across treatments are not drastically different. This overlap suggests that while certain treatments improve tensile strength, these improvements are not statistically significant enough to distinctly separate most treatments from one another. The variations in tensile properties are relatively small across treatments, with no single treatment consistently outperforming others by a large margin.

(**a**)



(**b**)

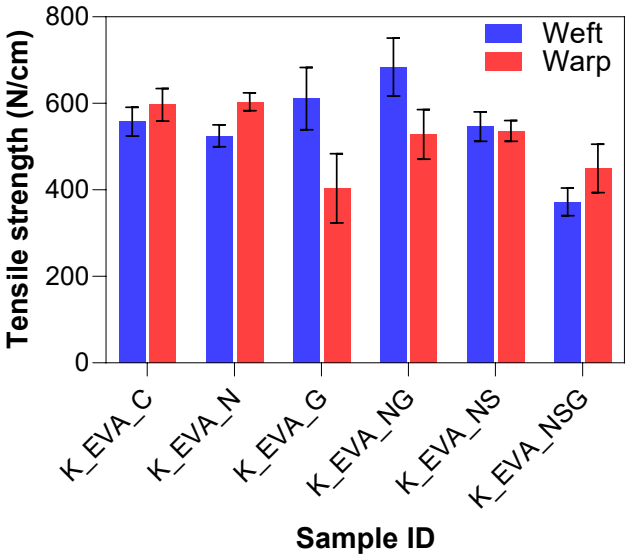


Figure 16. Tensile strength results of Kevlar laminates with (**a**) TPU matrix and (**b**) EVA matrix.

Table 7. Tukey–Kramer analysis of tensile strength for Kevlar laminates.

Level					
K_EVA_NG	A				
K_TPU_NS	A	B			
K_TPU_N	A	B			
K_EVA_C	A	B			
K_EVA_N	A	B			
K_EVA_NS	A	B	C		
K_EVA_G		B	C		
K_TPU_C		B	C	D	
K_TPU_G		B	C	D	
K_TPU_NG			C	D	E
K_TPU_NSG				D	E
K_EVA_NSG					E

3.4. Potential for Graphene NPs

Incorporating graphene nanoparticles into the fiber surfaces introduced a novel surface functionalization method. SEM analysis of UHMWPE seen in Figure 17a,b confirmed a significant amount of graphene particles deposited on the fiber surface. The images illustrate how the addition of graphene altered the surface texture, introducing a rougher, uneven profile compared to untreated UHMWPE fibers. This roughness may enhance interfacial adhesion in composite applications. However, despite the visible roughness due to graphene deposition, the woven structure and integrity of the UHMWPE fibers remain intact, indicating that the treatment does not compromise the bulk material properties. In the digital microscope images of UHMWPE (Figure 17c,d), you can clearly observe how the graphene particles are integrated into the fiber weave. The higher magnification (Figure 17d) revealed graphene particles embedded between individual UHMWPE filaments, suggesting that the treatment successfully targets inter-fiber regions, potentially increasing the overall surface area for bonding. The digital microscope images of Kevlar (Figure 17e,f) also show graphene particles on the surface, with higher agglomeration/deposition in specific regions. Graphene particles are also observed filling the gaps between the woven Kevlar fibers, enhancing inter-fiber bonding and reinforcing the Kevlar weave's structural integrity.

The graphene-treated fibers exhibited a notable increase in interfacial adhesion. The yarn pullout force increased by 18% for Kevlar and 12% for UHMWPE, suggesting that graphene's contribution comes from its ability to introduce additional functional groups capable of enhancing chemical bonding. FTIR analysis showed evidence of new C–C and C–O bonds, likely due to graphene's interaction with the fiber surface.

Interestingly, although the improvements in interfacial adhesion were not as pronounced as with the combined NaOH and silane treatment, graphene-treated fibers demonstrated enhanced tensile strength. The laminated composites containing graphene-treated Kevlar showed a 15% increase in tensile strength, while UHMWPE composites improved by 10%. This suggests that graphene can be effective in reinforcing the matrix–fiber interface, though further studies are needed to explore the full potential of combining graphene with other treatments. Graphene nanoparticles, while less established in the field of fiber-reinforced laminates, demonstrated potential for improving adhesion through chemical surface modification. The interaction between graphene and the fiber surface created new functional groups that improved bonding with the matrix. However, the effect was not as significant as traditional treatments like NaOH and silane. Regarding overall performance, the NaOH, silane, and graphene treatment was the most effective for Kevlar, while the plasma treatment showed the most significant promise for UHMWPE fibers. Graphene

nanoparticle treatment, though novel, provides a promising avenue for future research, particularly in combination with other surface treatments.

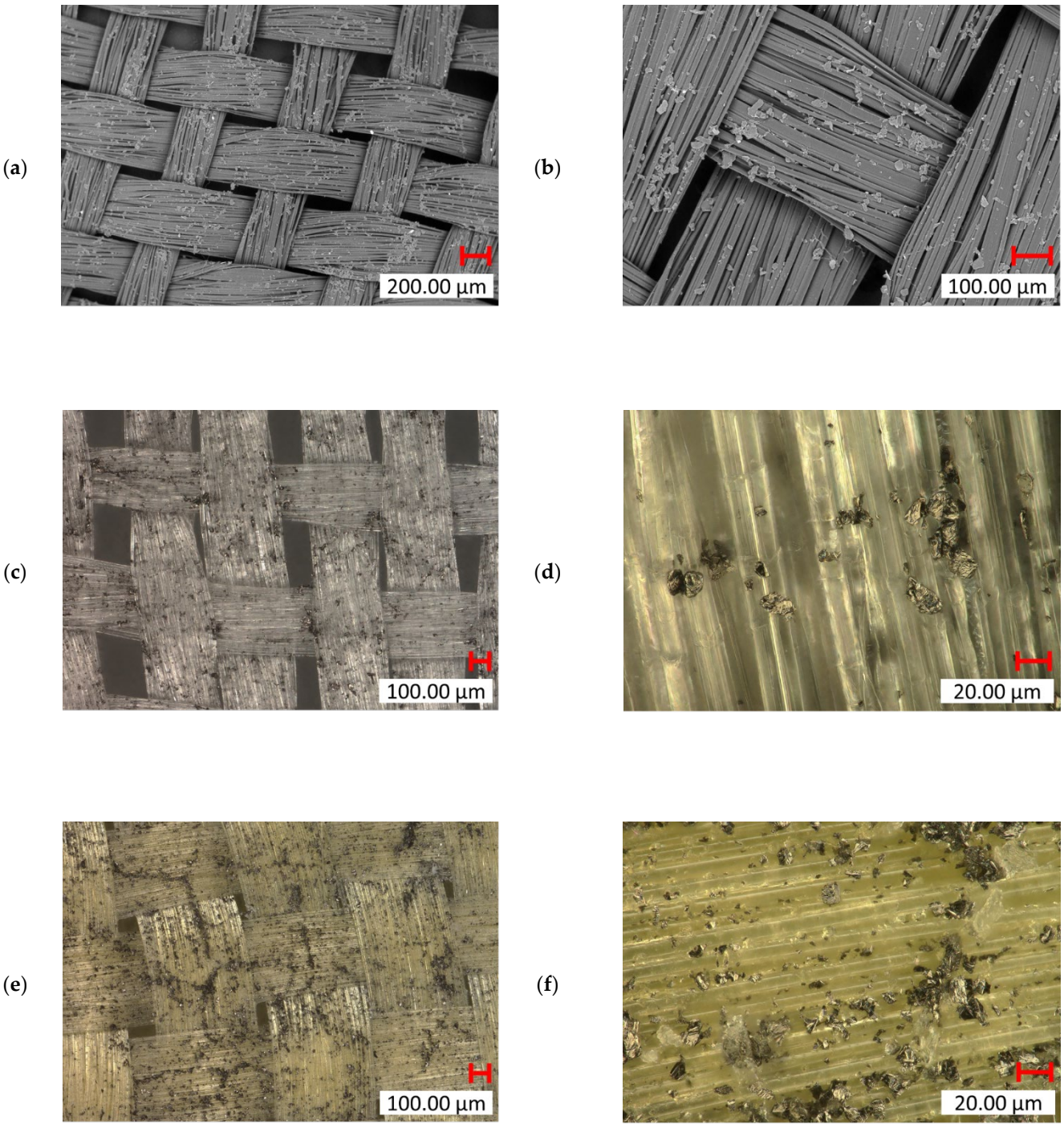


Figure 17. SEM (TM4000 15 kV) images of graphene NP-treated UHMWPE: (**a**) ×35 mag. and (**b**) ×100 mag; digital microscopic (Keyence VHX7000) images of graphene NP-treated UHMWPE: (**c**) ×100 mag. and (**d**) ×1000 mag.; and digital microscopic (Keyence VHX7000) images of graphene-treated Kevlar: (**e**) ×100 mag. and (**f**) ×1000 mag.

4. Conclusions

This study explored the effects of mechanical and chemical treatments on the interfacial adhesion and mechanical properties of Kevlar and UHMWPE fiber-reinforced laminates. The results confirmed that the performance of these treatments depends heavily on the

fiber type and matrix material. Mechanical roughening, chemical treatments, and the inclusion of nanomaterials all played significant roles in enhancing adhesion, with chemical modifications generally proving more effective than purely physical treatments.

For UHMWPE fibers, plasma treatment emerged as the most effective method for improving adhesion, particularly when paired with TPU as the matrix. Plasma treatment roughened the fiber surface and introduced new chemical functionalities, significantly enhancing bonding. The yarn pullout force for plasma-treated UHMWPE in TPU increased by 188.1%, highlighting the success of this approach for chemically inert fibers like UHMWPE. However, the combination of plasma and graphene, although offering some improvements over the control samples, did not surpass plasma treatment alone. This was attributed to the wet graphene treatment partially washing away the reactive chemical functionalities the plasma treatment introduced to the surface. The NaOH, silane (NS), and NaOH–silane–graphene (NSG) treatments were the most effective for Kevlar laminates, particularly in TPU matrices. The NSG-treated Kevlar/TPU samples exhibited the highest pullout force, with a 76.6% increase over the control, indicating a synergistic effect between surface roughening, chemical coupling, and nanomaterial reinforcement. Even in the EVA matrix, the NSG treatment led to a remarkable 95.4% increase in yarn pullout force, signifying the robustness of this combined treatment approach.

In contrast, graphene-only treatments resulted in more modest improvements, with increases of 8.2% for EVA and 9.7% for TPU matrices. While graphene nanoparticles introduced additional chemical functionalities and improved wettability, their effects were not as pronounced as the combined chemical treatments, suggesting that graphene is more effective when used with other surface modification techniques. The combined NaOH and silane treatment was particularly beneficial for Kevlar, which already has reactive groups. The chemical coupling facilitated by silane enhanced fiber–matrix bonding and significantly improved tensile strength and yarn pullout force, especially when combined with graphene. On the other hand, plasma treatment was more effective for UHMWPE, where its dual role of introducing chemical functionalities and roughening the fiber surface overcame UHMWPE's inherent chemical resistance. While our findings align with previous research [1,12–14,27,40,41], demonstrating that surface treatments that improve roughness or introduce functional groups significantly enhance interfacial bonding, we expanded the existing knowledge by specifically investigating the effects of graphene alone and in combination with established surface treatments. This research provides new insights into graphene's independent and synergistic roles in improving interfacial adhesion.

In conclusion, this study demonstrated that chemical modifications, particularly those that introduce functional groups (such as NaOH and silane), are more effective than purely mechanical treatments in enhancing the interfacial adhesion of fiber-reinforced laminates. Plasma treatment is especially beneficial for chemically inert fibers like UHMWPE, while combining NaOH, silane, graphene treatments was most effective for Kevlar, offering a powerful combination of surface roughening, chemical coupling, and nanomaterial reinforcement. Graphene nanoparticles present a promising new approach to surface functionalization, especially when combined with other treatments, and merit further exploration. While this study primarily relied on qualitative assessments of surface morphology using SEM, future work should integrate quantitative techniques such as atomic force microscopy (AFM) and profilometry to provide detailed insights into surface roughness parameters like average roughness (Ra) and root mean square roughness (Rq). Additionally, future investigations should explore the synergistic effects of combining multiple surface treatments, including plasma, silane, and nanomaterials, to enhance fiber–matrix bonding in high-performance composites. Further work could also focus on developing approaches to prevent the wet graphene treatment from partially washing away the reactive chemical

functionalities introduced by plasma treatment. This research opens new avenues for optimizing surface treatments tailored to the unique characteristics of different fiber and matrix combinations, ultimately advancing the development of stronger, more durable fiber-reinforced composites.

Author Contributions: Conceptualization, F.A. and A.-F.M.S.; Data curation, F.A.; Formal analysis, F.A.; Funding acquisition, A.-F.M.S.; Investigation, F.A. and J.G.; Methodology, F.A., J.G. and A.-F.M.S.; Project administration, A.-F.M.S.; Resources, J.G. and A.-F.M.S.; Software, F.A.; Supervision, J.G. and A.-F.M.S.; Validation, F.A., J.G. and A.-F.M.S.; Visualization, F.A. and J.G.; Writing—original draft, F.A.; Writing—review and editing, F.A., J.G. and A.-F.M.S. All authors have read and agreed to the published version of the manuscript.

Funding: This research received no external funding.

Data Availability Statement: The raw data supporting the conclusions of this article will be made available by the authors on request.

Conflicts of Interest: The authors declare no conflict of interest.

References

1. Faruk, O.; Yang, Y.; Zhang, J.; Yu, J.; Lv, J.; Lv, W.; Du, Y.; Wu, J.; Qi, D. A Comprehensive Review of Ultrahigh Molecular Weight Polyethylene Fibers for Applications Based on Their Different Preparation Techniques. *Adv. Polym. Technol.* **2023**, *2023*, 6656692. [CrossRef]
2. Chen, L.; Cao, M.; Fang, Q. Ballistic performance of ultra-high molecular weight polyethylene laminate with different thickness. *Int. J. Impact Eng.* **2021**, *156*, 103931. [CrossRef]
3. Abed, M.S.; Ahmed, P.S.; Oleiwi, J.K.; Fadhil, B.M. Low velocity impact of Kevlar and ultra high molecular weight polyethylene (UHMWPE) reinforced epoxy composites. *Multidiscip. Model. Mater. Struct.* **2020**, *16*, 1617–1630. [CrossRef]
4. Nael, M.A.; Dikin, D.A.; Admassu, N.; Elfishi, O.B.; Percec, S. Damage Resistance of Kevlar® Fabric, UHMWPE, PVB Multilayers Subjected to Concentrated Drop-Weight Impact. *Polymers* **2024**, *16*, 1693. [CrossRef]
5. Ansari, M.S.; Zafar, S.; Pathak, H. A comprehensive review of surface modification techniques for carbon fibers for enhanced performance of resulting composites. *Results Surf. Interfaces* **2023**, *12*, 100141. [CrossRef]
6. Li, H.; Hu, Y.; Fu, X.; Zheng, X.; Liu, H.; Tao, J. Effect of adhesive quantity on failure behavior and mechanical properties of fiber metal laminates based on the aluminum–lithium alloy. *Compos. Struct.* **2016**, *152*, 687–692. [CrossRef]
7. Li, A. *Evaluation of Laminated Hull Material for High Altitude Airship*; North Carolina State University: Raleigh, NC, USA, 2018.
8. Valadez-Gonzalez, A.; Cervantes-Uc, J.M.; Olayo, R.; Herrera-Franco, P.J. Effect of fiber surface treatment on the fiber–matrix bond strength of natural fiber reinforced composites. *Compos. Part B Eng.* **1999**, *30*, 309–320. [CrossRef]
9. Alshahrani, A.; Albaqami, M.; Naji, Z.; Al-Khunein, Y.; Alsubaie, K.; Alqahtani, A.; Al-Thobity, A.M. Impact of different surface treatment methods on bond strength between fiber post and composite core material. *Saudi Dent. J.* **2020**, *33*, 334–341. [CrossRef]
10. Mosharraf, R.; Ranjbarian, P. Effects of post surface conditioning before silanization on bond strength between fiber post and resin cement. *J. Adv. Prosthodont.* **2013**, *5*, 126–132. [CrossRef]
11. Liu, J.; Xue, Y.; Dong, X.; Fan, Y.; Hao, H.; Wang, X. Review of the surface treatment process for the adhesive matrix of composite materials. *Int. J. Adhes. Adhes.* **2023**, *126*, 103446. [CrossRef]
12. Li, M.; Ma, W.; Zhou, X. Surface modification of Kevlar fiber by nanoSiO_2 deposition in supercritical fluid. *Compos. Interfaces* **2018**, *26*, 857–870. [CrossRef]
13. Chowdhury, M.A.; Hossain, N.; Shuvho, B.A.; Kowser, A.; Islam, A.; Ali, R.; Ei-Badry, Y.A.; Ei-Bahy, Z.M. Improvement of interfacial adhesion performance of the kevlar fiber mat by depositing SiC/TiO_2/Al_2O_3/graphene nanoparticles. *Arab. J. Chem.* **2021**, *14*, 103406. [CrossRef]
14. Wu, X.; Zhan, L.; Zhao, X.; Wang, X.; Chang, T. Effects of surface pre-treatment and adhesive quantity on interface characteristics of fiber metal laminates. *Compos. Interfaces* **2019**, *27*, 829–843. [CrossRef]
15. Nejatbakhsh, S.; Anagri, A.; Omran, A.V.; Pulpytel, J.; Bazin, C.; Ullah, M.; Mirshahi, M.; Rezaie, H.; Javadpour, J.; Arefi-Khonsari, F. Improvement of the Bioactivity of UHMWPE by Two Different Atmospheric Plasma Treatments. *Plasma Chem. Plasma Process.* **2020**, *411*, 245–264. [CrossRef]
16. Teodoru, S.; Kusano, Y.; Rozlosnik, N.; Michelsen, P.K. Continuous Plasma Treatment of Ultra-High-Molecular-Weight Polyethylene (UHMWPE) Fibres for Adhesion Improvement. *Plasma Process. Polym.* **2009**, *6*, S375–S381. [CrossRef]
17. Silverstein, M.S.; Breuer, O.; Dodiuk, H. Surface modification of UHMWPE fibers. *J. Appl. Polym. Sci.* **1994**, *52*, 1785–1795. [CrossRef]

18. Chhetri, S.; Bougherara, H. A comprehensive review on surface modification of UHMWPE fiber and interfacial properties. *Compos. Part A Appl. Sci. Manuf.* **2021**, *140*, 106146. [CrossRef]
19. Liu, H.; Pei, Y.; Xie, D.; Deng, X.; Leng, Y.; Jin, Y.; Huang, N. Surface modification of ultra-high molecular weight polyethylene (UHMWPE) by argon plasma. *Appl. Surf. Sci.* **2010**, *256*, 3941–3945. [CrossRef]
20. Wu, G.M. Oxygen plasma treatment of high performance fibers for composites. *Mater. Chem. Phys.* **2004**, *85*, 81–87. [CrossRef]
21. Tamargo-Martínez, K.; Martínez-Alonso, A.; Montes-Morán, M.A.; Tascón, J.M.D. Effect of oxygen plasma treatment of PPTA and PBO fibers on the interfacial properties of single fiber/epoxy composites studied by Raman spectroscopy. *Compos. Sci. Technol.* **2011**, *71*, 784–790. [CrossRef]
22. Wen, Y.; Meng, X.; Liu, J.; Yan, J.; Wang, Z. Surface modification of high-performance polyimide fibers by oxygen plasma treatment. *High Perform. Polym.* **2016**, *29*, 1083–1089. [CrossRef]
23. Liu, H.; Xie, D.; Qian, L.; Deng, X.; Leng, Y.X.; Huang, N. The mechanical properties of the ultrahigh molecular weight polyethylene (UHMWPE) modified by oxygen plasma. *Surf. Coat. Technol.* **2011**, *205*, 2697–2701. [CrossRef]
24. Cheng, Z.; Li, B.; Huang, J.; Chen, T.; Liu, Y.; Wang, X.; Liu, X. Covalent modification of Aramid fibers' surface via direct fluorination to enhance composite interfacial properties. *Mater. Des.* **2016**, *106*, 216–225. [CrossRef]
25. Liu, N.; Wang, J.; Chen, B.; Han, G.; Yan, F. Enhancement on interlaminar shear strength and tribological properties in water of ultra high molecular weight polyethylene/glass fabric/phenolic laminate composite by surface modification of fillers. *Mater. Des.* **2014**, *55*, 805–811. [CrossRef]
26. Choi, J.D.; La Choi, Y.; Kim, H.S.; Seo, S.I.; Jeon, S.S.; Lee, H.M.; Jeong, B.C. Primary extraskeletal osteosarcoma of the seminal vesicle: A case report and literature review. *Annals* **2016**, *93*, e6–e8. [CrossRef]
27. Ramasamy; Arumugam, V.; Rajkumar, S. Surface modification of Kevlar fibre fabric and its influence on the properties of Kevlar/epoxy composites. *Bull. Mater. Sci.* **2019**, *42*, 173. [CrossRef]
28. Mihai, M.; Ton-That, M.-T. Novel bio-nanocomposite hybrids made from polylactide/nanoclay nanocomposites and short flax fibers. *J. Thermoplast. Compos. Mater.* **2017**, *32*, 3–28. [CrossRef]
29. Song, K. Interphase characterization in rubber nanocomposites. In *Progress in Rubber Nanocomposites*; Woodhead Publishing: Cambridge, UK, 2017.
30. Mohammadalipour, M.; Masoomi, M.; Ahmadi, M.; Kazemi, Z. The effect of simultaneous fiber surface treatment and matrix modification on mechanical properties of unidirectional ultra-high molecular weight polyethylene fiber/epoxy/nanoclay nanocomposites. *J. Compos. Mater.* **2018**, *52*, 2961–2972. [CrossRef]
31. Mohammadalipour, M.; Masoomi, M.; Ahmadi, M.; Safi, S. Interfacial shear strength characterization of GMA-grafted UHMWPE fiber/epoxy/nano clay hybrid nanocomposite materials. *RSC Adv.* **2016**, *48*, 41793–41799. [CrossRef]
32. Qiu, S.; Zhou, Y.; Waterhouse, G.I.; Gong, R.; Xie, J.; Zhang, K.; Xu, J. Optimizing interfacial adhesion in PBAT/PLA nanocomposite for biodegradable packaging films. *Food Chem.* **2021**, *334*, 127487. [CrossRef]
33. Tan, Z.; Li, W.; Huang, W. The effect of graphene on the yarn pull-out force and ballistic performance of Kevlar fabrics impregnated with shear thickening fluids. *Smart Mater. Struct.* **2018**, *27*, 075048. [CrossRef]
34. Lodh, F.P.; Gadhave, R.V.I. Reinforcing Effect of Graphene in Epoxy Adhesives: Review. *Open J. Compos. Mater.* **2024**, *14*, 60–70. [CrossRef]
35. Xu, H.; Zhang, X.; Yu, Y.; Yu, Y.; Weng, L. Enhanced adhesion property of epoxy resin composites through dual reinforcement mechanisms. *Next Mater.* **2024**, *3*, 100072. [CrossRef]
36. *ASTM D4157-13*; Standard Test Method for Abrasion Resistance of Textile Fabrics (Oscillatory Cylinder Method)1. ASTM International: West Conshohocken, PA, USA, 2022; pp. 1–4. [CrossRef]
37. Adekunle, F.; Li, A.; Vallubh, R.; Seyam, A.-F.M. Assessment of Adhesion in Woven Fabric-Reinforced Laminates (FRLs) Using Novel Yarn Pullout in Laminate Test. *J. Compos. Sci.* **2024**, *8*, 242. [CrossRef]
38. Adekunle, F.; Seyam, A.-F.M. The Effect of Adhesive Quantity on Adhesion Quality and Mechanical Characteristics of Woven Kevlar Fabric-Reinforced Laminated Structures. *J. Compos. Sci* **2024**, *8*, 505. [CrossRef]
39. *ASTM D5035*; Standard Test Method for Breaking Force and Elongation of Textile Fabrics (Strip Method). ASTM International: West Conshohocken, PA, USA, 2019.
40. Liu, Y.; Liang, G. Surface Modification and Interface Properties of Enzyme-mediated Grafting Kevlar Fibers. *Chin. J. Mater. Res.* **2015**, *29*, 794–800. [CrossRef]
41. Lin, M.-C.; Lou, C.-W.; Lin, J.-Y.; Lin, T.A.; Lin, J.-H. Structural improvement of laminated thermoplastic polyurethane/low-melting polyester/kevlar composites. *Polym. Compos.* **2018**, *40*, E550–E558. [CrossRef]

Disclaimer/Publisher's Note: The statements, opinions and data contained in all publications are solely those of the individual author(s) and contributor(s) and not of MDPI and/or the editor(s). MDPI and/or the editor(s) disclaim responsibility for any injury to people or property resulting from any ideas, methods, instructions or products referred to in the content.